Journal Pre-proof

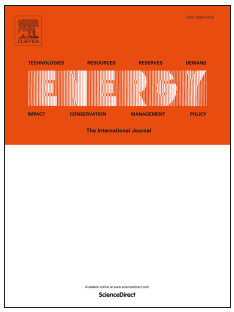

A multiobjective experimental based optimization to the CO_2 capture process using hybrid solvents of MEA-MeOH and MEA-water

Hamed Rashidi, Peyvand Valeh-e-Sheyda, Sasan Sahraie

PII: S0360-5442(19)32125-5

DOI: https://doi.org/10.1016/j.energy.2019.116430

Reference: EGY 116430

To appear in: *Energy*

Received Date: 12 June 2019

Revised Date: 23 October 2019

Accepted Date: 25 October 2019

Please cite this article as: Rashidi H, Valeh-e-Sheyda P, Sahraie S, A multiobjective experimental based optimization to the CO_2 capture process using hybrid solvents of MEA-MeOH and MEA-water, *Energy* (2019), doi: https://doi.org/10.1016/j.energy.2019.116430.

A multiobjective experimental based optimization to the CO_2 capture process using hybrid solvents of MEA-MeOH and MEA-water

Hamed Rashidi[a], Peyvand Valeh-e-Sheyda[a,*], Sasan Sahraie[a]

[a] Chemical Engineering Department, Kermanshah University of Technology, Kermanshah, Iran.

Abstract

To achieve the reduction of total energy consumption of CO_2 capture without the major drawbacks of conventional amine solvents, the superior performance of a blended physical-chemical solvent, MEA-MeOH, was experimentally compared with that of MEA aqueous absorbent in lab-scale absorption/desorption towers, equipped with stainless steel pall ring packings. Considering the typical industrial requirements, the main operating variables accounted for each solvent were the operating temperature (35-55 °C), amine concentration (15-30 wt%), gas flow rate (50-100 l/min), liquid flow rate (0.75-1.25 l/min), CO_2 concentration in the inlet gas (5-15 mol %), and the reboiler heat duty (1.4-2.2 kW). Response surface methodology was applied to give a quadratic mathematical model for obtained empirical volumetric overall mass transfer coefficients ($K_G a_V$). Based on the drastic increase of the energy requirement for solvent regeneration, a multiobjective optimization framework has been made to achieve the maximum desirable values for the $K_G a_V$, and the absorption percentage (Φ) with the minimum energy consumption (Ω). It was suggested that under the optimum operating condition, adding methanol to an aqueous MEA solution, reduces the regeneration energy consumption by 12%, while augmenting the CO_2 absorption percentage (Φ) by 9.1 %.

Keywords: Absorption, Box-Behnken, Carbon dioxide, hybrid, MEA-MeOH, MEA-H_2O.

1. Introduction

The global warming problem has been growing since the 1980s and the greenhouse gases are a clear cause for global warming according to the National Oceanic, and Atmospheric Administration (NOAA), [1]. Among all the greenhouse gases (GHGs), the amount of CO_2

* Corresponding author. Tel.: +98 8338305000; fax: +98 8338305006. *E-mail address:* p.valeh-sheyda@kut.ac.ir

released in the environment is much higher than the other greenhouse gases [2-4]. On the other side, the sustainability needs of today's society are stimulating the industry to develop the technologies that rapidly decline the emissions of carbon dioxide [5-8]. Among several technologies available for the CO_2 capture process, the post-combustion absorption of CO_2 with amine-based solvents is the most mature technology for industrial scales [9, 10]. However, developing novel efficient solvents that can provide rapid reaction kinetics, high absorption capacity, and low energy recovery for economic savings has created great challenges for the capture technology [11-13].

Today, the use of binary mixed alkanolamine solvents in optimal fraction ratios is of interest in CO_2 removal process of sour gases, due to the combined different physical and chemical properties, such as high absorption rate, low solvent vapor pressure, and low energy requirements [14-22]. The properties of hybrid solutions of amines as well as the experimental data in CO_2 removal processes have been proposed by several previous researches [15, 19, 23-25]. In summary, in hybrid solvents, favorable effects of physical solvents such as the high physical solubility of CO_2 at low CO_2 partial pressure, and the high separation performance with low regeneration energies has been combined with the high capacity advantages of chemical solvents. Recently, the hybrid solvent MEA-Methanol attracted more attention over aqueous MEA solvent, since it has a faster absorption rate to strip the same amount of CO_2 and a higher mass transfer rate compared with the MEA aqueous solvent [26]. So far, few studies have been conducted on the CO_2 capture in non-aqueous solutions of MEA and methanol [14-20].

Gao et al. [27] compared the carbon dioxide capture efficiency and the overall mass transfer performance of 30 wt% MEA-methanol and aqueous 30 wt% MEA solvents in a continuous liquid-gas absorption/desorption apparatus. Effects of key process parameters, namely the solvent flow rate at a constant flue gas flow rate, the flue gas flow rate, and the packing height on energy requirement have also been reported. In another study by Gao et al. [28] the effect of different operating conditions have been evaluated in an absorber packed with three different packings, namely Sulzer BX500, Mellapale Y500, and Pall rings 16-16. The results showed that the type of packing had a significant effect on the absorption efficiency of MEA-methanol solvent. In addition, they found that lean amine loading, lean amine flow rate, lean amine temperature, and inlet gas flow rate are the variables influencing the gas-phase volumetric

overall mass transfer coefficient and the absorption percentage [29]. Sema et al. [26] have compared the gas-phase volumetric overall mass transfer coefficient and the mass transfer flux of CO_2 absorption in three different solvents containing MEA-methanol, MEA-water, and MEA-methanol-water in a packed tower equipped with DX type structured packings. They found that the hybrid MEA-MeOH is to be more promising than two other solutions for CO_2 capture. Fu et al. [25] have also studied the effect of different operating conditions on the mass transfer performance CO_2 absorption efficiency in a double-layer glass packed tower. In this study, the potential effect of MEA-MeOH has been compared with MEA-water at an inlet liquid temperature of 10 °C. The studies on the effect of a hybrid water/ methanol solvent in the presence of MDEA and CO_2, at different operation temperatures indicated that MDEA aqueous solutions demonstrated lower performance than amine solutions using pure methanol or water–methanol mixtures as solvents, even at high temperatures and amine concentrations [30]. In another study, the CO_2 absorption in aqueous and hybrid solvents of MEA was investigated to explain the enhancement factor, as well as the kinetic rate between CO_2 and MEA-methanol hybrid solvent [31]. It is well demonstrated that the CO_2 absorption performance of any hybrid alkanolamines does not inevitably have a linear relation with the performance of their parent alkanolamines. As such, the assessment of their performance is particularly crucial due to the unsystematic behavior of these blended solvents.

Reviewing the literature on hybrid MEA-methanol systems, reveals that previous studies examined the impact of several operating conditions and design parameters on the cost of post-combustion CO_2 capture [32, 33]. The development of technological innovations on the absorption performance of MEA-Methanol illustrates that there are some gaps in previous researches. First, the optimization problem of the hybrid system has not been extensively discussed in all of the aforementioned studies. That is to say, no rigorous process model was developed for the aforementioned physical-chemical hybrid solvent to find the optimal operating conditions, energy and cost requirements. Second, no systematic research has accounted for the combined effects of operating variables on the overall performance of CO_2 absorption. This means that the optimization of a single parameter does not individually reflect the interactive effects of operating variables since the effect of one independent process parameter inevitably relies on the other parameters. Third, the absorption performance is not the only parameter that affects the operating cost of an industrial CO_2 absorption process. Even more significant is the

fact that the energy requirement of the post-combustion CO_2 capture process is extremely high until now. From the practical point of view, to obtain satisfactory capture efficiency with a minimum cost of CO_2 removal in the actual operation, the overall absorption performance must be simultaneously optimized with the required energy consumption during the solvent regeneration. Consequently, development of the promising solvents must be exerted along with an advanced multiobjective optimization framework of the CO_2 capture process to design the optimal CO_2 absorption process for the hybrid physical-chemical solvent.

In this study, an attempt has been made to employ the response surface methodology (RSM) for CO_2 capture process; to be specific, a general validity rule was numerically investigated to compare the potential of hybrid MEA-MeOH with that of traditional aqueous MEA solution in terms of CO_2 capture, and energy consumption in a packed absorption/desorption bed. For this purpose, the process scheme was designed based on the process operating conditions of industrial needs at atmospheric pressure. The experiments were conducted at an operating temperature of 45-65 °C, a solvent flow rate of 0.5- 1.25 l/min, an amine concentration range of 15-30 wt%, a gas flow rate of 50-100 l/min, a reboiler heat duty of 1.4-2.2 kW, and an inlet CO_2 concentration of 5-15 mol%. The mass transfer performance was ultimately evaluated in terms of the gas-phase volumetric overall mass transfer coefficient as the response variable. Besides, under the optimal operating condition, the potentials of the two blended solutions were compared regarding the gas-phase volumetric overall mass transfer coefficient, absorption percentage, and energy consumption. The experimental data and process optimization developed in this study are useful for industrial operating conditions typically encountered.

2. Materials and Methods

2.1. Chemicals

In this study, sulfuric acid, and sodium sulfate with a minimum purity of 98% and 99%, both were supplied by Kimia Pars Company, Iran. HCl was prepared from Merck-Schuchardt. Methanol was obtained from Shiraz Petrochemical Company, Iran with a purity >99%. MEA of purity >99% has been purchased from Shazand Arak Petrochemical Company, Iran and was used

as purchased without further purification. Methyl orange used for experiments was supplied from French BioChem Company.

2.2. Chemical Reactions

The chemical absorption of CO_2 in both aqueous and non-aqueous solutions of primary amines is a two-step reaction, which mainly comprises the well-established zwitterion mechanism [26, 34-39]. As expressed by reactions 1-3, in the first step, the reaction of CO_2 with amine produces an intermediate called a zwitterion. In the second step, the zwitterion is converted to a carbamate ion through deprotonation of the zwitterions.

Step 1: Formation of a zwitterion:

$$CO_2 + RNH \leftrightharpoons RNH_2^+CO_2^- \quad (1)$$

Step 2: Deprotonation of zwitterion and formation of carbamate ion:

$$RNH_2^+CO_2^- + B \leftrightharpoons RNHCO_2^- + BH^+ \quad (2)$$

where RNH is MEA and B represents water, methanol, OH^-, MEA or any base existing in the solution. The overall reaction is given by the sum of reactions (1) and (2), leading to the reaction (3), as follows:

$$CO_2 + RNH + B \leftrightharpoons RNHCO_2^- + BH^+ \quad (3)$$

The general reaction of CO_2 with MEA is an equilibrium and reversible reaction [31].

2.3. Experimental

2.3.1. Experimental apparatus

A schematic diagram of the gas absorption/desorption process, as well as the experimental setup used in this work, are depicted in Fig.1. The absorption unit is also composed of a random packed column, fresh solvent tank, a bubbling flask, three calibrated flow meters, a liquid-flow distributor, and a CO_2 analyzer. The absorption process was carried out in the packed column,

containing two packing beds, which was made of plexiglass with a grade of 10-12. The geometrical characteristics of the absorption/desorption unit have been provided in Table 1. The bubbling flask was applied to saturate the gas mixture with the solvent vapor. The saturated gas flow is introduced into the bottom of the counter-current absorber, below the packing section. Flow meters provide a direct measurement of liquid and gas entering the column. A liquid-flow distributor has also been provided at the top of each consecutive packed section to uniformly distribute the solvent on the packing surface. To avoid losses of the volatile absorbent, the outlet gas from the absorber is sent directly to a condenser and a scrubber. Besides, the fresh solvent tank supplies the make-up solvent, since the absorbent losses in the absorption column.

In the next step, the stripper is regarded as well. The rich solvent from the absorber bottom is first heated in a plate heat exchanger and then introduced to the top of the regeneration column. The stripper of the apparatus was made of 304 stainless steel pipe with an internal diameter of 10.7 cm. The column was filled with stainless steel Pall rings of 16×16 mm. The regenerated absorbent from the desorption tower is then cooled with the rich solvent and an additional heat exchanger before its returning to the absorber top. The overhead gaseous stream from the stripper is recovered to the process by using a condenser.

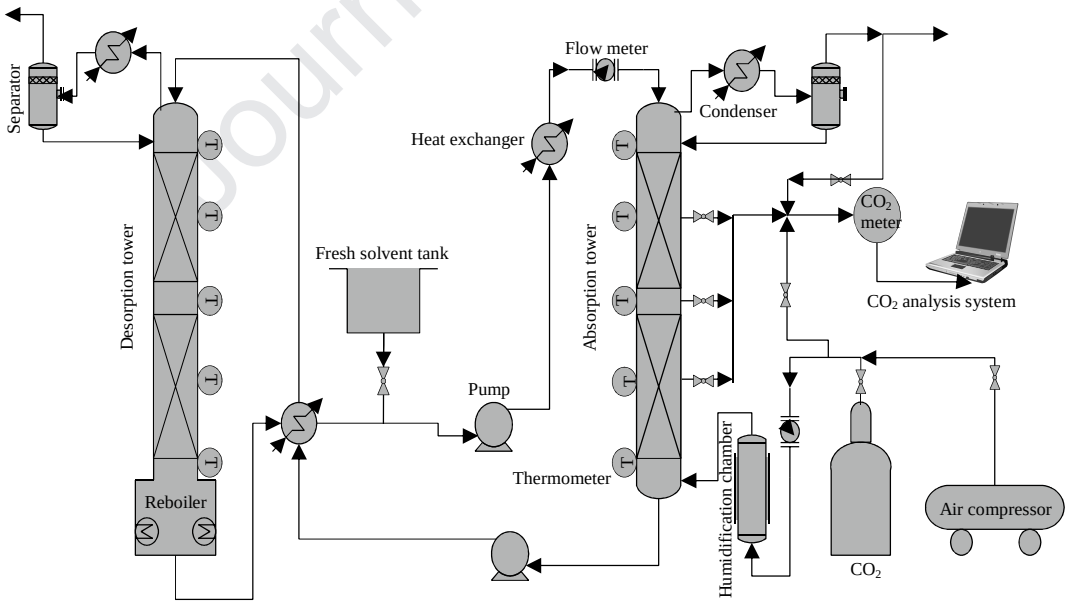

b)

Fig. 1. The experimental setup of gas absorption apparatus: a) The flow sheet, b) The actual setup.

To monitor the temperature during the experiments, the absorber and stripper have been equipped with five temperature sensors, installed along the sides of the tower at regular intervals. Besides, three gas samplers were placed along the absorber column at the top, bottom, and middle of the absorption beds to withdraw the CO_2 content of the samples. A digital CO_2 analyzer has continuously measured the CO_2 concentration of the gas-phase. All of the required measurements were computer-assisted and continuously logged on a PC. Details on CO_2 capture instruments applied to measure and analyze materials and variables in the CO_2 capture experiments can be found in our previous work [40].

Table 1. Specification of the CO_2 absorption experimental setup

Absorption tower height	2 m
Diameter absorption tower	9.7 cm
Desorption tower height	2 m
Diameter desorption tower	10.7 cm
Pressure absorption tower	atmospheric
Pressure desorption tower	atmospheric
Inlet gas temperature	ambient temperature (27 °C)
Packing type	Pall ring stainless steel 16×16 mm

2.3.2. Absorption experiments

Prior to the experiments, it is necessary to investigate a suspected gas leakage in all parts of the setup. The absorption experiments were initialized by pumping the solvent to the absorber top. The absorbent, charged from a storage tank, has been set at desired flow rates. The column was heated and operated at experimental conditions until the liquid was stabilized to the desired temperature. Then, the gas mixture was prepared by controlling the gas flow rates of pure carbon dioxide and compressed air before re-mixing. The prepared CO_2-air gas mixture was introduced to the bottom of the column. Once a steady-state condition was achieved for both gas and liquid, the CO_2 concentrations in gas stream has been measured at the inlet and outlet of the column. Besides, the absorber temperature was gathered along the absorption tower. Zeng et al. have proposed a relatively simplified correlation model for determination of overall mass transfer coefficient, $K_G a_v$ in the packed column [41]. The description of the defined correlation can be found elsewhere and will only be briefly summarized here [25, 40].

In this work, the absorption performance of CO_2 has been evaluated in terms of $K_G a_V$ in kmol/m^3.h.kPa, the absorption percentage (Φ), and the energy consumption of the regenerator (Ω) from the following equations:

$$\phi = \frac{\dot{n}_{CO_{2,in}} - \dot{n}_{CO_{2,out}}}{\dot{n}_{CO_{2,in}}} \tag{4}$$

$$K_G a_V = \frac{G}{ZP}\left[\ln\left(\frac{Y_{in}}{Y_{out}}\right) + (Y_{in} - Y_{out})\right] \tag{5}$$

$$Y = \frac{y}{1-y} \tag{6}$$

$$\Omega = \frac{Q}{m_{CO_2}} \tag{7}$$

where $\dot{n}_{in}$ and $\dot{n}_{out}$ denote the molar flow of the gas at the bottom and top of the absorption column, respectively. $K_G a_V$, has been computed based on the gas-phase volumetric overall mass transfer coefficient. The variables in Eq. 5 were also measured from the absorption experiments; Y_{in} and Y_{out} present the solute-free concentrations in feed and exit gas, which is commonly called the mole ratio of CO_2 in feed and exit gas. y, which is measured by CO_2 sensor during the experiment, indicate the mole fraction of CO_2 in the gas phase. P, Z, and G are the system pressure (kPa), the height of absorption bed (m), and the inlet gas flow rate (kmol/h.m^2), respectively [26]. Moreover, Q and m are the energy consumed by the reboiler (MJ) and the CO_2 captured (kg), respectively.

2.3.2. Box-Behnken experimental design

It is recognized that some process variables are as key variables for CO_2 capture systems in terms of the impact it ultimately has on the assessment of the plant performance and economic merit. An attempt has been carried out to build the range of process variables close to the typical ranges of operating variables for common industrial plants. A six-factor, three-level Box-Behnken factorial design (BBD) was generated to estimate for six variables in the following ranges: temperature (T= 35-55°C), gas flow rate (G-F=50-100 l/min), liquid flow rate (L-F=0.75-1.25 l/min), inlet CO_2 concentration (C-CO_2=5-15 %), reboiler heat duty (Q=1.4-2.2 kW), and amine concentration (C-MEA=15-30 %). Table 2 illustrates the complete list of experiments defined for the six-factor three-levels Box-Behnken design in terms of coded and real values of the

parameters. The design of experiments and response values were analyzed using Design Expert 11.0. (trial version). As shown in Table 3, the BBD matrixes of 54 experiments cover the full design of six factors for building regression models. The experimental data achieved from the BBD model experiments can be represented in the form of the following equation:

$$Y = \beta_0 + \sum_{i=1}^{n} \beta_i X_i + \sum_{i=1}^{n} \beta_{ii} {X_i}^2 + \sum_{i=1}^{n-1} \sum_{j=i+1}^{n} \beta_{ij} X_i X_j \qquad i, j = 1, 2, 3 \qquad (8)$$

where Y is the predicted response variable ($K_G a_V$), n determines the number of independent variables. X_i and X_j represent the uncoded or actual variables; β_0 is an independent parameter based on the mean value of the experimental setup; β_i, β_{ii}, and β_{ij} are regression coefficients that measures the effects of linear, quadratic, and interaction terms of variables, respectively; i and j reflect the index numbers for factor [42, 43].

Table 2. BBD matrix of experiments with the experimental and predicted response values for two solvents (T= temperature, C-CO_2= inlet CO_2 concentration, G-F= gas flow rate, L-F=liquid flow rate, Q= reboiler heat duty, C-MEA= amine concentration)

Test No.	actual level of variables						Response					
	T (°C)	C-CO_2 (vol.%)	G-F (l/min)	L-F (l/min)	Q (kW)	C-MEA (wt.%)	Observed K_Ga_V (kmol/m^3.h.kPa)		Predicted K_Ga_V(kmol/m^3.h.kPa)		Relative error (%)	
							MEA-water	MEA-MeOH	MEA-water	MEA-MeOH	MEA-water	MEA-MeOH
1	35	5	75	0.75	1.8	22.5	1.32	1.77	1.52	1.64	15.15	7.34
2	55	5	75	0.75	1.8	22.5	1.32	1.9	1.34	1.87	1.52	1.58
3	35	15	75	0.75	1.8	22.5	1.10	1.7	0.97	1.3	11.82	23.53
4	55	15	75	0.75	1.8	22.5	0.90	1.38	0.79	1.33	12.22	3.62
5	35	5	75	1.25	1.8	22.5	1.89	2.87	1.94	3.3	2.65	14.98
6	55	5	75	1.25	1.8	22.5	1.80	2.64	1.76	2.63	2.22	0.38
7	35	15	75	1.25	1.8	22.5	1.54	2.3	1.39	2.05	9.74	10.87
8	55	15	75	1.25	1.8	22.5	1.17	1.71	1.21	1.38	3.42	19.30
9	45	5	50	1	1.4	22.5	0.93	1.45	1.01	1.57	8.60	8.28
10	45	15	50	1	1.4	22.5	0.72	1.19	0.46	1.33	36.11	11.76
11	45	5	100	1	1.4	22.5	1.84	3.1	1.75	2.8	4.89	9.68
12	45	15	100	1	1.4	22.5	1.21	2.29	1.20	1.56	0.83	31.88
13	45	5	50	1	2.2	22.5	1.70	2.88	1.74	3.19	2.35	10.76
14	45	15	50	1	2.2	22.5	1.18	2.07	1.19	1.95	0.85	5.80
15	45	5	100	1	2.2	22.5	1.60	2.52	1.72	3.42	7.50	35.71
16	45	15	100	1	2.2	22.5	1.20	2.04	1.17	2.18	2.50	6.86
17	45	10	50	0.75	1.8	15	0.60	0.95	0.60	0.68	0.00	28.42
18	45	10	100	0.75	1.8	15	0.80	1.18	0.73	0.91	8.75	22.88
19	45	10	50	1.25	1.8	15	0.93	1.67	1.02	1.44	9.68	13.77
20	45	10	100	1.25	1.8	15	1.23	2.26	1.15	1.67	6.50	26.11
21	45	10	50	0.75	1.8	30	1.93	4.11	1.96	4.59	1.55	11.68
22	45	10	100	0.75	1.8	30	2.61	4.85	2.55	4.82	2.30	0.62
23	45	10	50	1.25	1.8	30	2.42	5.38	2.38	5.35	1.65	0.56
24	45	10	100	1.25	1.8	30	3.00	5.45	2.97	5.58	1.00	2.39
25	35	10	75	0.75	1.4	22.5	0.88	1.47	1.01	1.53	14.77	4.08
26	55	10	75	0.75	1.4	22.5	0.90	1.36	0.83	0.86	7.78	36.76
27	35	10	75	1.25	1.4	22.5	1.40	2.4	1.43	2.29	2.14	4.58
28	55	10	75	1.25	1.4	22.5	1.20	1.91	1.25	1.62	4.17	15.18
29	35	10	75	0.75	2.2	22.5	1.33	1.89	1.36	2.15	2.26	13.76
30	55	10	75	0.75	2.2	22.5	1.33	1.79021	1.18	1.48	11.28	17.33
31	35	10	75	1.25	2.2	22.5	1.82	2.59	1.79	2.91	1.65	12.36
32	55	10	75	1.25	2.2	22.5	1.64	2.25	1.60	2.24	2.44	0.44
33	45	5	75	1	1.4	15	0.85	1.64	0.79	1.58	7.06	3.66
34	45	15	75	1	1.4	15	0.92	1.55	1.12	1.62	21.74	4.52
35	45	5	75	1	2.2	15	1.10	1.76	0.96	1.23	12.73	30.11
36	45	15	75	1	2.2	15	1.12	1.78	1.29	2.57	15.18	44.38
37	45	5	75	1	1.4	30	3.19	8.05	3.08	7.11	3.45	11.68
38	45	15	75	1	1.4	30	1.61	3.05	1.64	3.28	1.86	7.54
39	45	5	75	1	2.2	30	4.03	10.35	3.61	8.69	10.42	16.04
40	45	15	75	1	2.2	30	2.10	4.96	2.17	4.87	3.33	1.81
41	35	10	50	1	1.8	15	0.72	1.05	0.60	1.27	16.67	20.95
42	55	10	50	1	1.8	15	0.62	1.02	0.52	0.85	16.13	16.67
43	35	10	100	1	1.8	15	0.61	1.13	0.48	1.06	21.31	6.19
44	55	10	100	1	1.8	15	0.92	1.71	0.90	1.6	2.17	6.43
45	35	10	50	1	1.8	30	2.33	8.12	2.32	6.95	0.43	14.41
46	55	10	50	1	1.8	30	1.44	2.12	1.52	2.99	5.56	41.04
47	35	10	100	1	1.8	30	2.51	4.37	2.65	5.66	5.58	29.52
48	55	10	100	1	1.8	30	2.26	3.83	2.36	4.74	4.42	23.76
49	45	10	75	1	1.8	22.5	1.12	1.53	1.12	1.47	0.00	3.92
50	45	10	75	1	1.8	22.5	1.10	1.53	1.12	1.47	1.82	3.92
51	45	10	75	1	1.8	22.5	1.10	1.53	1.12	1.47	1.82	3.92
52	45	10	75	1	1.8	22.5	1.11	1.51	1.12	1.47	0.90	2.65

53	45	10	75	1	1.8	22.5	1.09	1.53	1.12	1.47	2.75	3.92
54	45	10	75	1	1.8	22.5	1.10	1.53	1.12	1.47	1.82	3.92

3. Results and discussion

3.1. Temperature and CO_2 concentration profiles along the absorption column

Fig.2a displays gas-phase CO_2 concentration profile along the column for MEA-H_2O and MEA-MeOH. As seen, 10 mol% of CO_2 in the feed gas was absorbed by the blended test solvents within 140 cm packed bed height. Although both MEA-H_2O and MEA-MeOH could provide nearly a similar trend for CO_2 absorption, the superior performance of MEA-MeOH can be differentiated by comparing the absorption performance at a similar column height. Totally, for all ratios of L/G=8.57, 11.43, and 17.15, MEA-H_2O gave the lowest CO_2 absorption performance compared to the MEA-MeOH. As an illustration, for a constant ratio of L/G=8.57, MEA-H_2O could absorb about 50 % of inlet CO_2 within 70 cm of the packed bed from the top, while at the same height, MEA-MeOH offered a higher absorption of 62 %.

Besides, to extend the performance comparisons, the absorption experiments were conducted at different liquid to gas ratios. As expected, an increase in L/G boosts the driving force resulting in increasing of the overall mass transfer, and overall absorption. For instance, as the ratio of the L/G increased from 8.57 to 17.15, the absorption performance of MEA-MeOH has been improved from 81 % to 94.8 %. Finally, a high CO_2 absorption performance of 95 % was achieved at L/G= 17.15 for MEA-MeOH.

Fig. 2b shows the absorber temperature profile along the length of the column. As illustrated, the exothermic reaction between CO_2 and the solvent results in a steep temperature increase at constant L/G ratio. This behavior is mainly the result of the consecutive heat transfers between the solvent and gas streams in the packed bed [44]. Generally, for all test solutions, as L/G increases from 8.57 to 17.15, the maximum temperature is pushed toward the rich end of the tower, and the location of the temperature bulge moves toward the bottom of the column, meaning the main absorption rate will be at the bottom of the tower. This is mainly due to the fact that at high ratios of L/G, the MEA-H_2O solvent has carried more heat due to its relatively higher heat capacities, compared with MEA-MeOH. As such, the reaction mostly occurs at the

bottom section of the column, and the peak of the temperature bulge shifted slightly down in the absorption column [45, 46].

Furthermore, the comparison of two test solutions clearly reveals that in the case of MEA-MeOH solution, the location of the temperature bulge has shifted to the top of the packed bed and becomes more distinct. This may be due to the overall higher absorption rate of the employed MeOH compared to H_2O under atmospheric pressure, resulting in a slightly more temperature drop at the bottom of the packed bed.

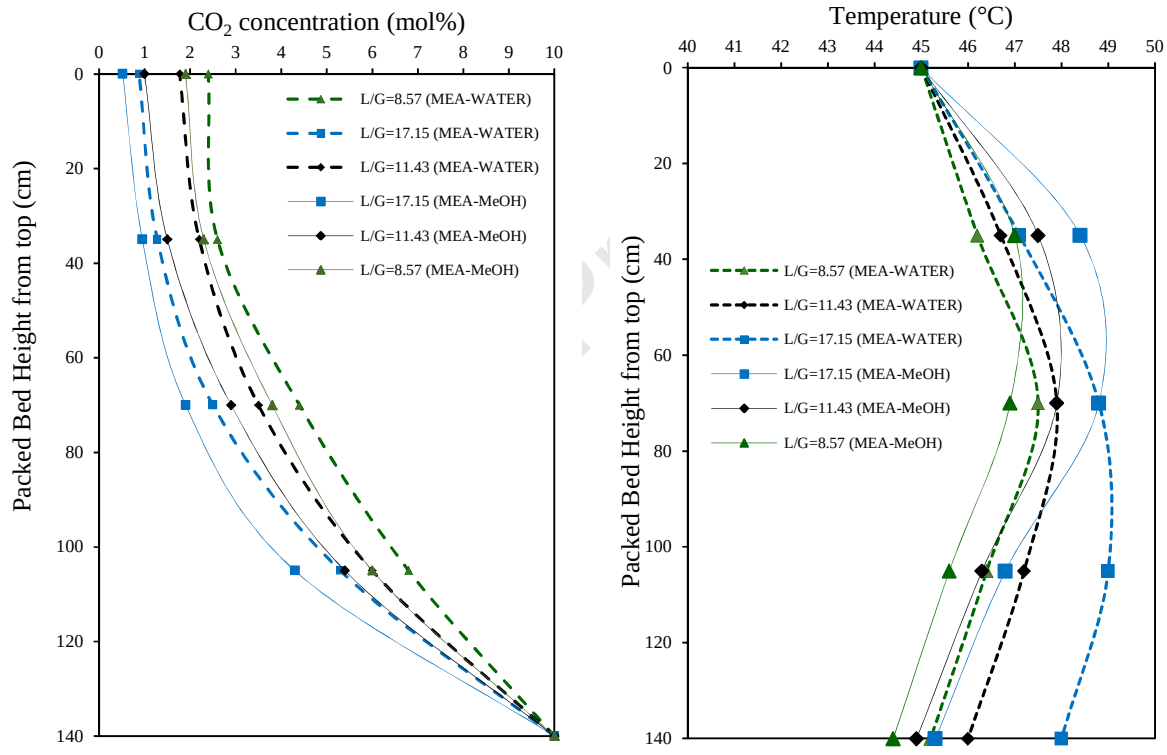

(*a*) (*b*)

Fig. 2. Profile of (a) CO_2 concentration in the gas phase (b) temperature along the absorption column (temperature of the inlet solvent = 45 °C, CO_2 concentration in the inlet gas = 10%, solvent flow rate = 1 l/min, reboiler heat duty = 1.8 kW and amine concentration = 30 wt%)

3.2. Amine loading along the absorption column

Fig. 3 shows the amine loading profile along the absorption tower. According to the figure, as the absorption column increased from 0 to 140 cm, the CO_2 loading of both solutions leaving the absorption column, was varied from 0.36 to 0.46 mol/mol. Furthermore, with increase the packed bed height, the CO_2 loadings shifted toward the right, resulting in higher amount of CO_2 to be absorbed. The reason is that increasing the absorber height rises the feed solvent residence time, which enhances the CO_2 recovery.

The corresponding reboiler heat duties were further evaluated at different CO_2 loadings. The results suggest that the blended solution of MEA-MeOH behaves somewhat differently from MEA-H_2O. For instance, within 140 cm height of the column, the CO_2 loading in aqueous solution of MEA was increased from 0.11 to 0.37 mol/mol at reboiler heat duty of 1.4 kW, while in the case of MEA-MeOH, the CO_2 loading has raised from 0.27 to 0.46 mol/mol at the same reboiler heat duty. Considering the high vaporization heat and the heat capacity of water in comparison with methanol, MEA-MeOH is rather sensitive to the reboiler heat duty than MEA-H_2O, offering less amine loading in the lean MEA solution. It is noticeable that when the lean loading is high, more solvent is needed to be circulated to capture the same amount of CO_2 [47]. Consequently, superior absorption performance of MEA-MeOH is expected over MEA-H_2O.

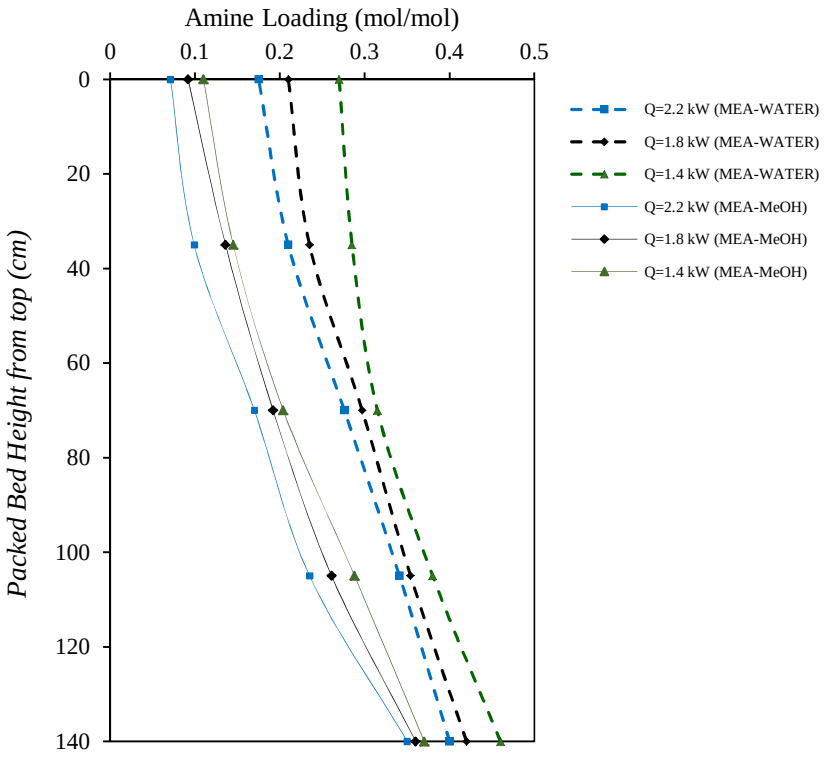

Fig. 3. Amine loading profile along the absorber (temperature of the feed solvent = 45 °C, CO_2 concentration in the inlet gas = 10%, gas flow rate = 75 l/min, solvent flow rate = 1 l/min, and amine concentration = 30 wt%)

3.3. Gas-phase volumetric overall mass transfer coefficient along the absorption column

The gas-phase volumetric overall mass-transfer coefficient ($K_G a_V$) is a lumped parameter that considers the absorption performance per unit volume of the packed column. Fig. 4 demonstrates the $K_G a_V$ along the height of the absorber. It is apparent that under experimental conditions, the $K_G a_V$ values for MEA-MeOH are higher than that for MEA-H_2O, illustrating the better potential of MEA-MeOH for the CO_2 absorption. The reason can be explained by the low values of Henry's constant for CO_2 in methanol compared with that for water. As studied by previous researchers, a low Henry's constant means a large driving force for mass transfer leading to higher CO_2 loading at the gas-liquid interface [32]. Furthermore, for both experiment runs, the values of the $K_G a_V$ firstly increased to a maximum at the height of 1.05 m from the bottom of the

packed column and then decreased along the height of the absorber. Based on this, the increase in height of the absorption column from 1.05 to 1.4 does not provide an increase in the absorption capacity of CO_2. The value of the Z in Eq. 5 also represents the great impact of the absorption height on the gas-phase volumetric overall mass transfer coefficient.

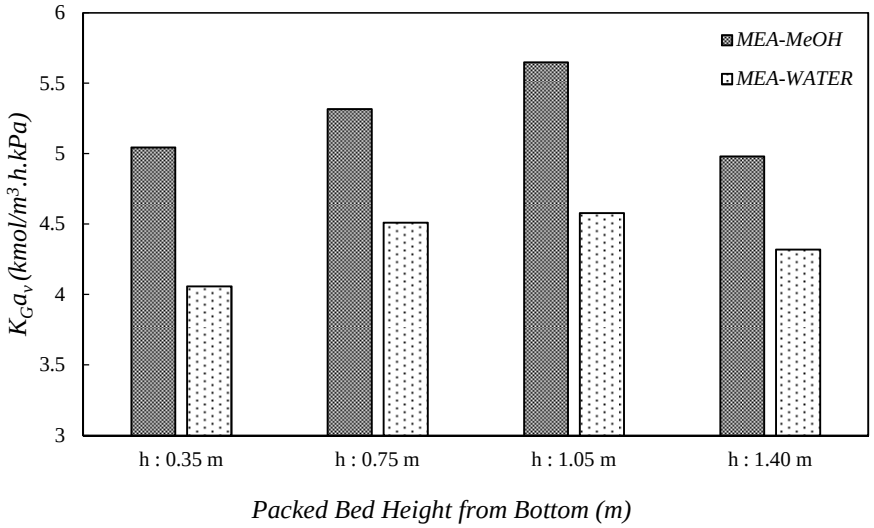

Fig. 4. The gas-phase volumetric overall mass transfer coefficient at the height of the absorption tower (temperature of the feed solution = 45 °C, CO_2 concentration in the inlet gas = 5%, gas flow rate = 100 l/min, solvent flow rate = 1.25 l/min, reboiler heat duty = 2.2 kW and amine concentration = 30 wt%)

3.4. Statistical analysis

The accuracy of the employed polynomial model, as well as the statistical significance of the variables, have been verified by Analysis of variance (ANOVA). The values of the ANOVA and the significance of the regression coefficients in both absorption experiments are listed in Tables 3 and 4.

From the results, it is observed that the model F-values obtained for the overall mass transfer coefficient (81.54 and 27.52) are higher than the Fisher's F-value ($F_{0.05,\ 18,\ 35}$=1.91 and $F_{0.05,13,40}$=1.97). Accordingly, it is concluded that the quadratic regression model is significant for the gas-phase volumetric overall mass transfer coefficient. Furthermore, the corresponding p-

values in the ANOVA table (< 0.0001) clearly revealed that the developed model is statistically significant. However, the lack of fit is not statistically significant at 95 % confidence level. The significant linear, quadratic, and interaction terms were also specified for both under-studied absorbont at the 5% level.

Table 3. ANOVA results for $K_G a_V$ under MEA-water absorbent

Sources	SS	DF	MS	F-value	P-value	
Model	24.95	18	1.39	81.54	< 0.0001	significant
A:T	0.2017	1	0.2017	11.86	0.0015	significant
B:C-CO2	1.83	1	1.83	107.73	< 0.0001	significant
C:G-F	0.7812	1	0.7812	45.95	< 0.0001	significant
D:L-F	1.07	1	1.07	62.75	< 0.0001	significant
E:Q	0.742	1	0.742	43.64	< 0.0001	significant
F:C-MEA	15.14	1	15.14	890.32	< 0.0001	significant
AC	0.1275	1	0.1275	7.5	0.0096	significant
AF	0.2556	1	0.2556	15.03	0.0004	significant
BF	1.57	1	1.57	92.14	< 0.0001	significant
CE	0.2926	1	0.2926	17.21	0.0002	significant
CF	0.2025	1	0.2025	11.91	0.0015	significant
EF	0.0648	1	0.0648	3.81	0.0589	significant
A^2	0.0645	1	0.0645	3.79	0.0596	significant
B^2	0.2418	1	0.2418	14.22	0.0006	significant
C^2	0.0773	1	0.0773	4.54	0.0401	significant
D^2	0.309	1	0.309	18.18	0.0001	significant
E^2	0.092	1	0.092	5.41	0.0259	significant
F^2	2.24	1	2.24	131.99	< 0.0001	significant
Residual	0.5951	35	0.017			
Lack of Fit	0.5432	30	0.0181	0.1757	0.31	not significant
Pure Error	0.0519	5	0.0103			
Cor Total	25.55	53				

Table 4. ANOVA results for K_Ga_V under MEA-methanol absorbent

Sources	SS	DF	MS	F-value	P-value	
Model	172.1	13	13.24	27.52	< 0.0001	significant
A:T	2.69	1	2.69	5.6	0.0229	significant
B:C-CO2	9.26	1	9.26	19.26	< 0.0001	significant
C:G-F	0.3083	1	0.3083	0.6409	0.4281	significant
D:L-F	3.44	1	3.44	7.14	0.0108	significant
E-Q	2.29	1	2.29	4.77	0.0349	significant
F-C-MEA	91.81	1	91.81	190.86	< 0.0001	significant
AC	4.61	1	4.61	9.57	0.0036	significant
AF	6.28	1	6.28	13.06	0.0008	significant
BF	13.31	1	13.31	27.68	< 0.0001	significant
EF	1.86	1	1.86	3.87	0.0561	significant
B^2	2.63	1	2.63	5.46	0.0246	significant
E^2	1.87	1	1.87	3.89	0.0555	significant
F^2	34.5	1	34.5	71.73	< 0.0001	significant
Residual	19.24	40	0.481			
Lack of Fit	18.98	35	0.5422	10.42	0.27	not significant
Pure Error	0.26	5	0.052			
Cor Total	191.34	53				

Applying quadratic regression analysis for the experimental data obtained during the running of BBD, the second-order polynomial models are given as follows:

$$K_Ga_{V(MEA\text{-}water)} = + 0.931146 + 0.077833\ T + 0.087583\ C\text{-}CO_2 + 0.026217\ G\text{-}F - 4.70333\ L\text{-}F - 0.929167\ Q - 0.141528\ C\text{-}MEA + 0.000505\ T \times G\text{-}F - 0.002383\ T \times C\text{-}MEA - 0.011800\ C\text{-}CO_2 \times C\text{-}MEA - 0.019125\ G\text{-}F \times Q + 0.000600\ G\text{-}F \times C\text{-}MEA + 0.030000\ Q \times C\text{-}MEA - 0.000792\ T^2 + 0.006133\ C\text{-}CO_2{}^2 - 0.000139\ G\text{-}F^2 + 2.77333\ L\text{-}F^2 + 0.591146\ Q^2 + 0.008304\ C\text{-}MEA^2 \quad (9)$$

$$K_Ga_{V(MEA\text{-}methanol)} = + 17.38002 + 0.004751\ T + 0.258852\ C\text{-}CO_2 - 0.132042\ G\text{-}F + 1.51330\ L\text{-}F - 12.12479\ Q - 0.478330\ C\text{-}MEA + 0.003035\ T \times G\text{-}F - 0.011817\ T \times C\text{-}MEA - 0.034400\ C\text{-}CO_2 \times C\ –MEA + 0.160833\ Q \times C\text{-}MEA + 0.019545\ C\text{-}CO_2{}^2 + 2.57750\ Q^2 + 0.029452\ C\text{-}MEA^2 \quad (10)$$

The predicted values of the gas-phase volumetric overall mass transfer coefficients for MEA-water and MEA-methanol, are calculated from Eqs. 9 and 10, as presented in Table 2. Based on the table, the values of the average relative error are estimated around 6.6% and 13.2% for MEA-water and MEA-methanol, which are almost acceptable for model validation.

The adequacy of the regression models has been estimated in Fig. 5, using the diagnostic plots. From the experimental values of the response versus the predicted values, it is found that there are tendencies in the linear regression fit and the preferred model sufficiently describes the experimental range examined. The fit of the models were also controlled by the coefficient of determination, R^2, adjusted determination, adj-R^2, and predicted R^2. The high values of obtained coefficients for both models illustrate that the real association between the response and independent variables is satisfactory, as reported in the figures.

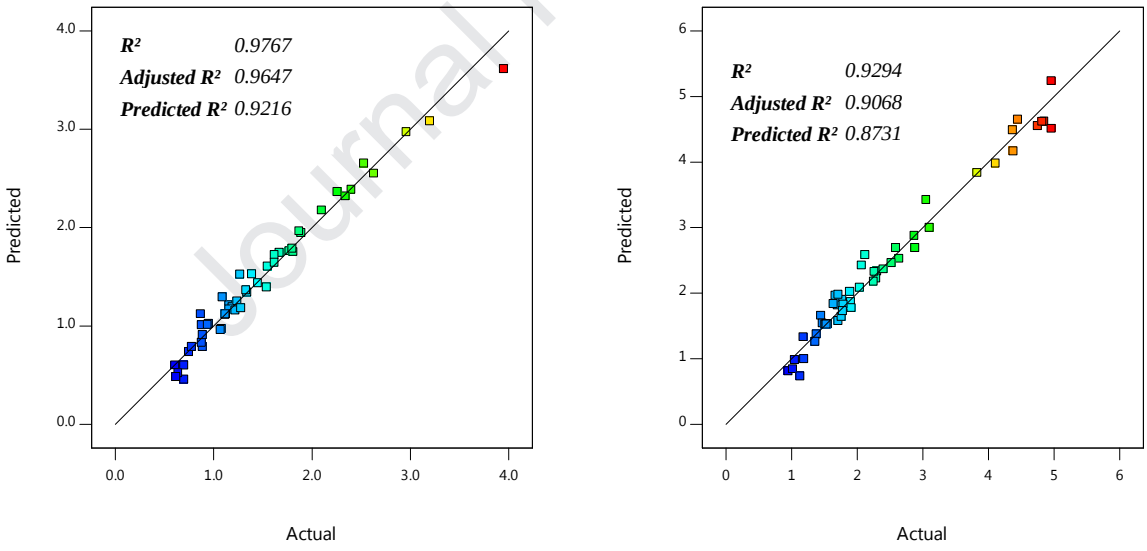

(a) (b)

Fig. 5. The actual and predicted response values: a) MEA-water, b) MEA- methanol

3.5. Parametric analysis of the CO_2 absorption efficiency

Based on the second-order polynomial model obtained from the BBD, the main linear factors known as the main challenges for the factual employment of the absorption process and had the strongest impact on the predicted values of the gas-phase volumetric overall mass transfer coefficients were analyzed for MEA-MeOH and MEA-water. Also, to assess the MEA-MeOH's potential for the CO_2 absorption, its absorption performance has been compared in terms of $K_G a_V$ with that of aqueous MEA solution.

3.5.1. Effect of inlet solvent temperature

The linear effect of the inlet temperature of the blended amine solutions was plotted in Fig. 6. It is found that for MEA-H_2O, the $K_G a_V$ begins from 1.1 kmol/ m^3.h.kPa for solvent temperature of 35°C, then reaches a maximum at temperature of 45 °C. At this stage, the effect of temperature was noticed to improve the overall mass transfer coefficient. At higher temperatures, such increasing trend of $K_G a_V$ has not been seen; as the temperature increases from 45 to 55 °C, it plateaus, but the decline is small.

For aqueous solution of MEA, it is reasonable to assume that the CO_2 absorption by the MEA-H_2O combines the chemical and physical absorption. In the chemical absorption, the inlet liquid temperature is directly linked with the reaction rate according to the Arrhenius equation [48]. In the view of molecular dynamics, the reaction rate constantly increases with increasing temperature. Besides, the high viscosity of the 22.5 % MEA solution adversely influences the diffusion process. Instead, increasing the temperature simply reduces the solvent viscosity, which leads to the enhancement of the absorption rate. However, in the physical absorption, the CO_2 solubility in the liquid phase can be explained according to Henry's law, corresponding to a reduction in the solubility of CO_2 into a liquid due to the temperature increase [49-51].

This trend was not followed by MEA-MeOH; as seen in the figure, the $K_G a_V$ is reduced constantly by increasing the temperature from 35 to 55°C. The physical absorption seems to be dominant rather than chemical absorption. The positive effect of methanol was also reduced especially at higher temperatures, since the solvent evaporation from the liquid phase to the gas phase reduces the values of the flow density values, N_A (kmol/m^2.s). Finally, the low values of

Henry's constant in CO_2-MEA-MeOH system compared with CO_2-MEA-H_2O correspond to the higher CO_2 concentration in the gas-liquid interface. Consequently, the driving force of the mass transfer, and thereby the physical CO_2 solubility is increased in CO_2-MEA-MeOH.

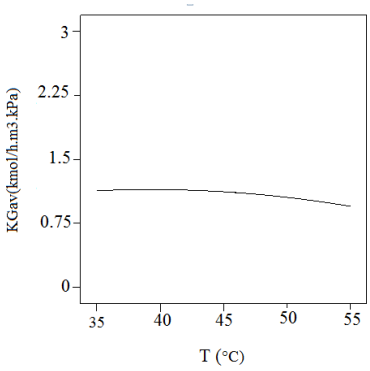

(I)

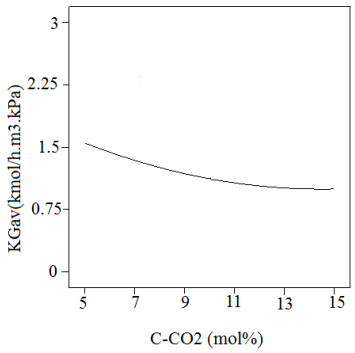

(II)

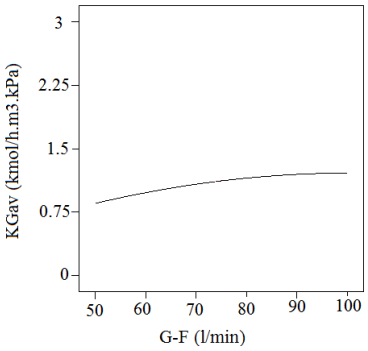

(III)

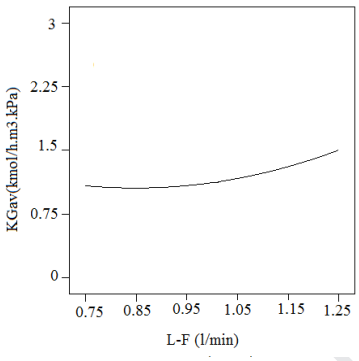

(IV)

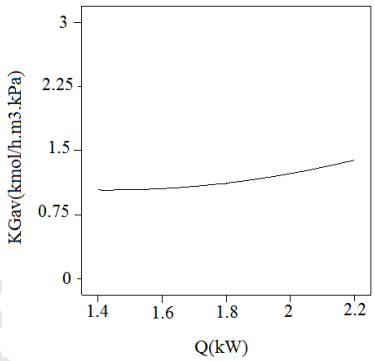

(V)

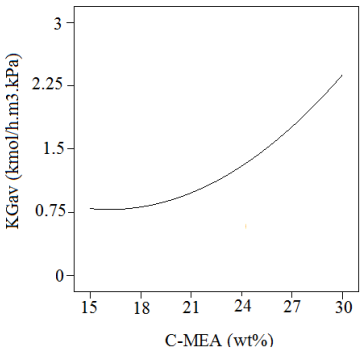

(VI)

(a)

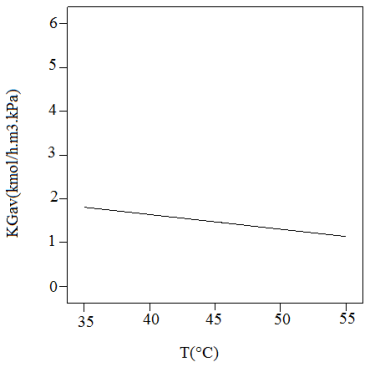

(I)

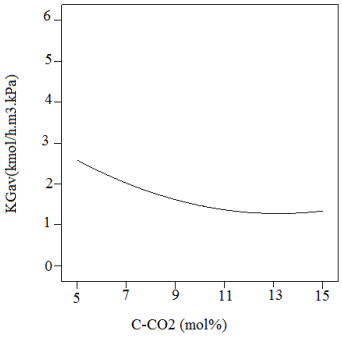

(II)

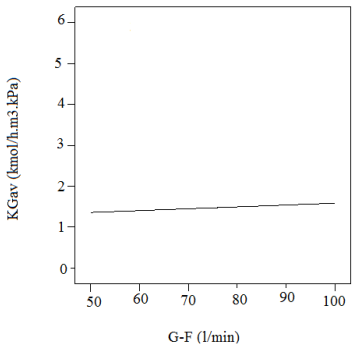

(III)

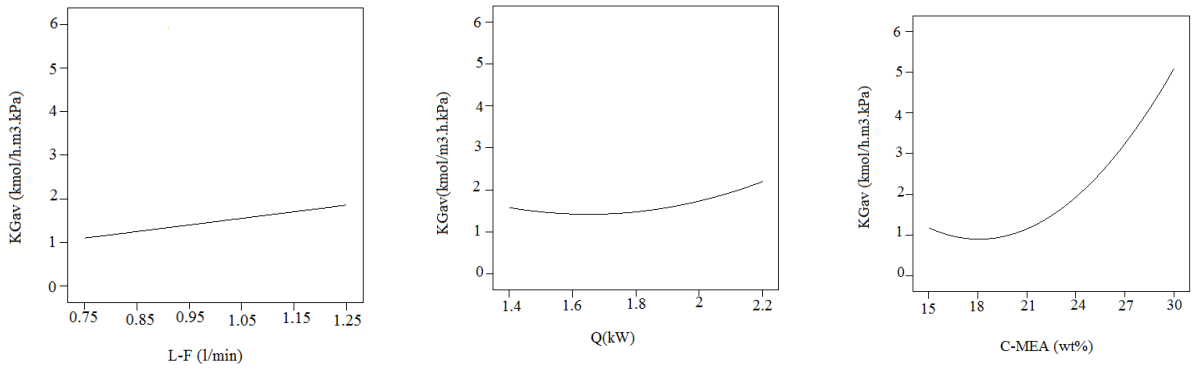

(IV) (V) (VI)

(b)

Fig. 6. Variation of the $K_G a_V$ with operational variables for a) MEA-H_2O, b) MEA-MeOH (T= temperature, C-CO_2= inlet CO_2 concentration, G-F= gas flow rate, L-F=liquid flow rate, Q= reboiler heat duty, C-MEA= amine concentration)

3.5.2. Effect of CO_2 concentration in the inlet gas

The mass transfer performance for both hybrid solvents was predicted in terms of the inlet CO_2 concentration and the $K_G a_V$ in Fig. 6. As seen, the changes in the CO_2 concentration at the inlet from 5 to 15 mol%, have negative effects on the gas-phase overall mass transfer coefficient. The reduction in the $K_G a_V$ results from the mass transfer driving force. Normally, by increasing in the CO_2 inlet concentration, more CO_2 molecules travel from gas bulk to the gas-liquid interface, promoting an increase of CO_2 pressure. Logically, the increase in CO_2 partial pressure would consume more active free MEA molecules in the solution, resulting in decreasing the overall gas-phase mass transfer coefficient. This phenomenon implies that the rate of gas absorption does not exclusively rely on the mass transfer phenomenon in the gas phase; the resistance of the liquid phase also plays a dominant role on the mass transfer behavior of the CO_2 absorption in hybrid alkanolamine solutions. The other studies have also revealed similar results [25, 41].

3.5.3. Effect of inlet gas flow rate

Fig. 6 predicts the values of the $K_G a_V$ under different ranges of gas flow rate from 50 to 100 l/min. It is found that (1) for both hybrid solvents, the inlet gas flow rate, has a minor effect on

the gas-phase overall mass transfer coefficient quantitatively; (2) for MEA-H_2O, an increase in the inlet gas flow rate affects the gas-phase overall mass transfer coefficient positively. However, at high gas flow rates of 100 l/min, it almost remains at a constant value of 1.3 kmol/ m^3.h.kPa; (3) for MEA-MeOH, there is a similar trend of increasing $K_G a_V$ with increasing inlet gas flow rate, but generally more linearly.

Based on the mass transfer theory of the gas-liquid reaction, increasing the gas flow rate gives rise to the value of the $K_G a_V$. Furthermore, Eq. 5 shows the direct effect of the gas flow rate on the gas-phase volumetric overall mass transfer coefficient. On the other side, increasing the gas flow rate decreases the residence time of the gaseous phase in the absorption column, thereby, increases the CO_2 concentration at the bottom of the column. As such, the combination of these two contributions suggests the direct dependencies of the $K_G a_V$ values with the inlet gas flow rate entering to the column.

3.5.4. Effect of inlet solvent flow rate

The parametric effect of the liquid flow rate on the $K_G a_V$ has been demonstrated in Fig. 6, when the other variables are constant. Based on the figure, $K_G a_V$ is found to enhance for both blended solutions, when the liquid flow rate increased from 0.75 to 1.25 l/min. This can be explained according to the two-film theory; increasing the solvent flow rate will not only provide more actively available sites for CO_2 absorption but will also be beneficial to the effective interfacial area of gas-liquid (a_V) in the absorption column. On the other sides, increasing the solvent flow rate results in a higher liquid-side mass transfer coefficient (k_L), which is associated with the enhancement of the K_G value [52]. Previous studies on the CO_2 absorption in have reported the same trend of the $K_G a_V$ increasing with the solvent flow rate in the packed column [25, 41, 53-56].

Comparing the values of the $K_G a_V$ in studied hybrid solutions indicate that the use of MEA-MeOH solution significantly reduces the amount of circulating mixture solution compared to the MEA-H_2O solution, which directly affects the removal costs of the CO_2 capture process. The detailed reasons have been discussed previously in Section 3.3.

3.5.5. Effect of reboiler heat duty

The main contributions to the regeneration energy requirement are specified by the heat duty of the reboiler. Fig. 6 depicts the variation of the gas-phase overall mass transfer coefficient in terms of the reboiler heat duty for the two hybrid solvents over the ranges of 1.4-2.2. kW. It is noticed that the heat duty values directly affect the $K_G a_V$ values. This can be described by the fact that the loading of the lean amine solution from the evaporator outlet is rather sensitive to the heat duty of the reboiler. In other words, if the heat duty of the strip tower for CO_2 desorption is increased, the loading of the lean amine will be decreased. Reducing the amine loading entering the absorption tower will increase the active sites; consequently, the values of the $K_G a_V$ are expected to rise.

The trends of the lean amine loading, as well as the comparison of the corresponding values of the $K_G a_V$ in terms of the reboiler heat duty have been illustrated in details, for MEA-H_2O and MEA-MeOH, in Fig. 7. It can be observed that when MEA-MeOH is implemented, at the minimum requirement of the reboiler heat duty (1.4 kW), the gas-phase volumetric overall mass transfer coefficient is 1.54 kmol/m^3.h.kPa. However, nearly the same value of $K_G a_V$=1.41 kmol/m^3.h.kPa is achieved at the maximum allowable value of the reboiler heat duty (2.2 kW) for MEA-H_2O solution. As a whole, the experimentally observations showed that for all ranges of the reboiler heat duties from 1.4 to 2.2 kW, the use of MEA-MeOH solution instead of the MEA-H_2O solution increases the gas-phase overall mass transfer coefficient from 33% to 38 %.

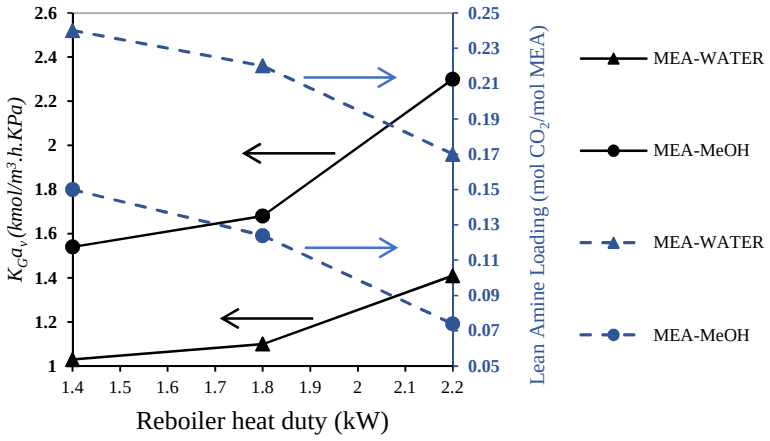

Fig. 7. Comparison of gas-phase volumetric overall mass transfer coefficient and lean amine loading under different reboiler heat duty

3.5.6. Effect of amine concentration

Fig. 6 displays the effect of initial amine concentration, ranging from 15 to 30 wt %, on the predicted values of the $K_G a_V$. As seen, the $K_G a_V$ has experienced an increase with increasing amine concentration in the aqueous solution of MEA, following the similar behavior as noticed for the fresh blended mixture of MEA-MeOH. This is because the driving force during the mass transfer is supplied by the available reactive alkanolamine concentration. As such, the number of active sites for chemical absorption of CO_2 significantly increases with the amount of MEA in the solvent.

However, MEA-H_2O offers lower values of the $K_G a_V$ than MEA-MeOH. For instance, at MEA concentration of 30 wt %, the $K_G a_V$ values of MEA-MeOH were higher than those of MEA-H_2O. As explained before, this may be because the difference between Henry's law constant of CO_2 in MeOH and H_2O.

3.6. Effect of interactive variables

The ultimate objective of BBD method utilized in this study was to display the significant interaction terms, specified in the ANOVA results in Tables 3 and 4 for CO_2 capture from the hybrid solvent of MEA-H_2O and MEA-MeOH. In Figs. 8 and 9, the predicted response for the gas-phase volumetric overall mass transfer coefficient were represented graphically to visualize the shape of the response surface.

Generally, for both blended solutions, the contours displayed a complex interaction between the process variables. As an illustration, From Fig. 8a, it is seen that the maximum value of the $K_G a_V$=3 kmol/h.m^3.kPa can be achieved for MEA-H_2O at the minimum temperature, and amine concentration in the solvent when the other operational variables are set to the middle values. The same interaction is true for CO_2 concentration in the inlet gas and initial amine concentration in Fig. 8d; at the lowest CO_2 concentration of 5 mol %, $K_G a_V$ is strongly influenced by raising the initial amine concentration from 15 to 30 wt %. However, problems associated with the device corrosion, as well as an excessive increase in viscosity by increase in MEA concentration must be considered as the limiting factors [57-59].

In Fig. 8c, it is recognized that the $K_G a_V$ value has increased to the peak with the increase in gas flow rate and reboiler heat duty up to 100 l/min and 2.2. kW. At maximum flow rate of 100 l/min, the change in reboiler heat duty does not have any significant effect on the mass transfer increase. Based on this study, it is also possible to obtain high values of $K_G a_V$, at the maximum reboiler heat duty for all ranges of the gas flow rate from 50 to 100 l/min. This also reveals the unique role of reboiler heat duty in in CO_2 absorption experiments. On the other sides, the rapid increase in both pairs of variables including reboiler heat duty, and amine concentration (Fig. 8e) and/or gas flow rate and amine concentration (Fig. 8f) significantly enhance the achieved values of volumetric overall mass transfer coefficient.

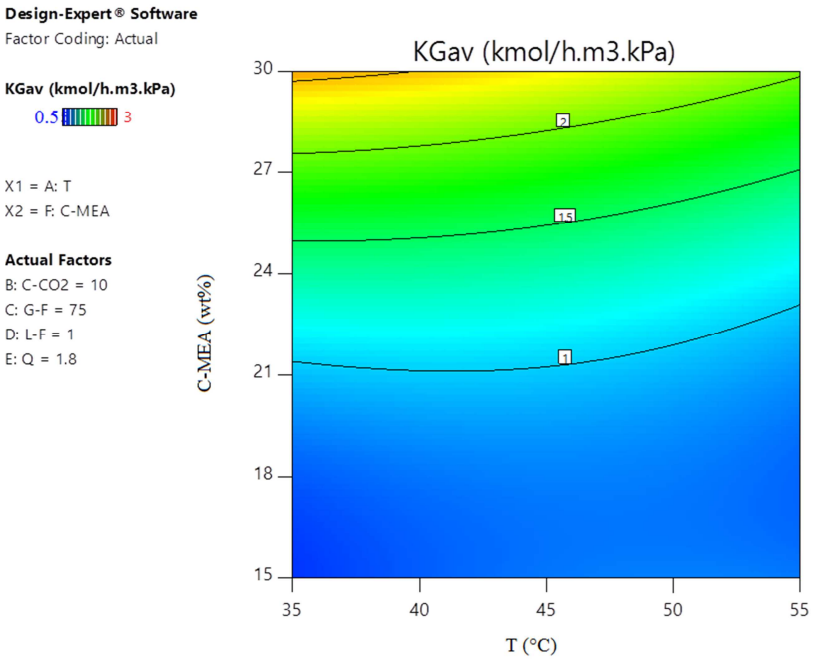
Design-Expert® Software
Factor Coding: Actual
KGav (kmol/h.m3.kPa)
0.5
3
X1 = A: T
X2 = F: C-MEA
Actual Factors
B: C-CO2 = 10
C: G-F = 75
D: L-F = 1
E: Q = 1.8
KGav (kmol/h.m3.kPa)
C-MEA (wt%)
T (°C)
30
27
24
21
18
15
35
40
45
50
55
2
1.5
1

(a)

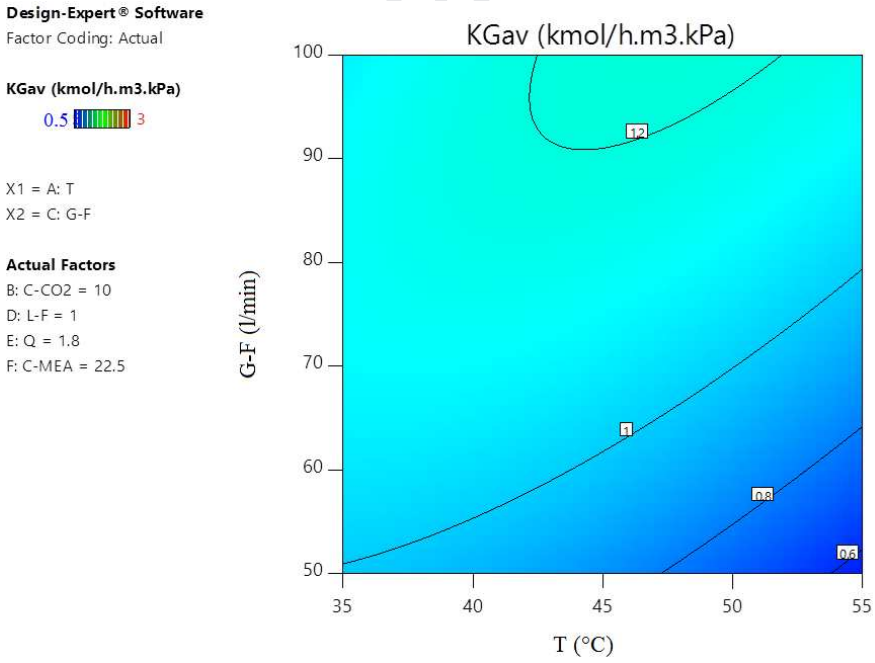
Design-Expert® Software
Factor Coding: Actual
KGav (kmol/h.m3.kPa)
0.5
3
X1 = A: T
X2 = C: G-F
Actual Factors
B: C-CO2 = 10
D: L-F = 1
E: Q = 1.8
F: C-MEA = 22.5
KGav (kmol/h.m3.kPa)
G-F (l/min)
T (°C)
100
90
80
70
60
50
35
40
45
50
55
1.2
1
0.8
0.6

(b)

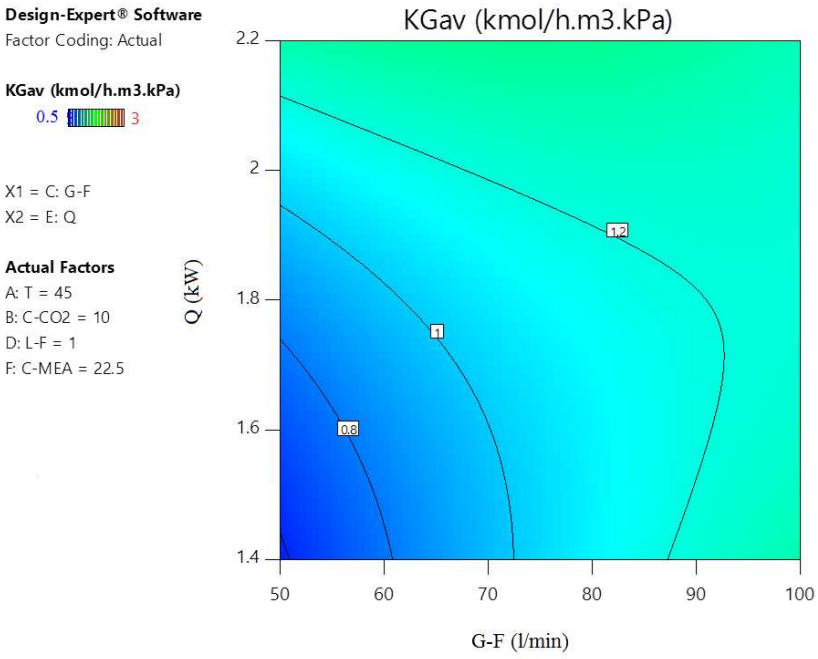
Design-Expert® Software
Factor Coding: Actual
KGav (kmol/h.m3.kPa)
0.5
3
X1 = C: G-F
X2 = E: Q
Actual Factors
A: T = 45
B: C-CO2 = 10
D: L-F = 1
F: C-MEA = 22.5
KGav (kmol/h.m3.kPa)
Q (kW)
G-F (l/min)
2.2
2
1.8
1.6
1.4
50
60
70
80
90
100
1.2
1
0.8

(c)

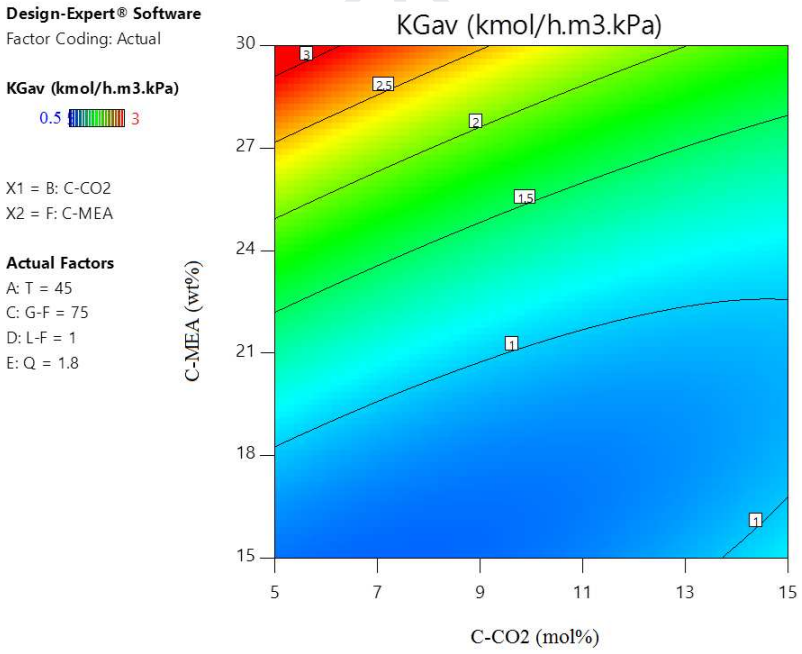
Design-Expert® Software
Factor Coding: Actual
KGav (kmol/h.m3.kPa)
0.5
3
X1 = B: C-CO2
X2 = F: C-MEA
Actual Factors
A: T = 45
C: G-F = 75
D: L-F = 1
E: Q = 1.8
KGav (kmol/h.m3.kPa)
C-MEA (wt%)
C-CO2 (mol%)
30
27
24
21
18
15
5
7
9
11
13
15
3
2.5
2
1.5
1

(d)

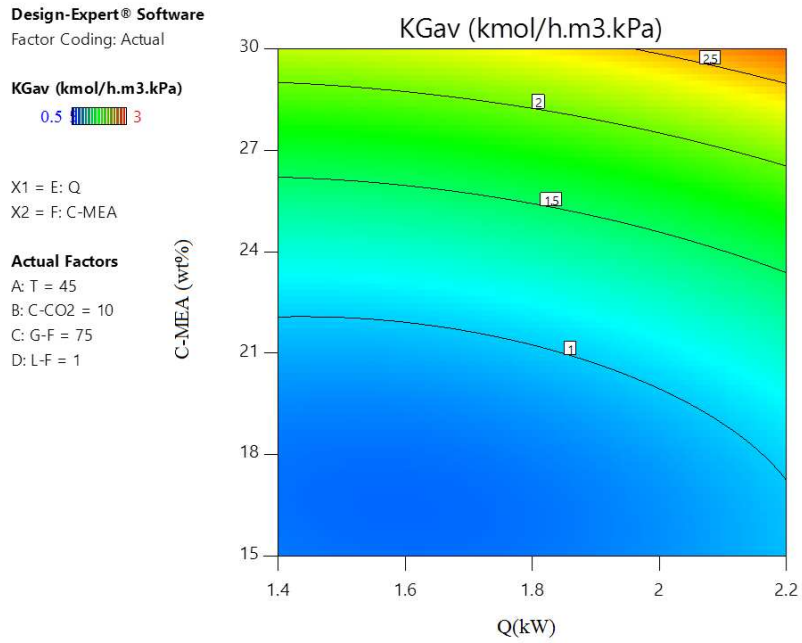

(e)

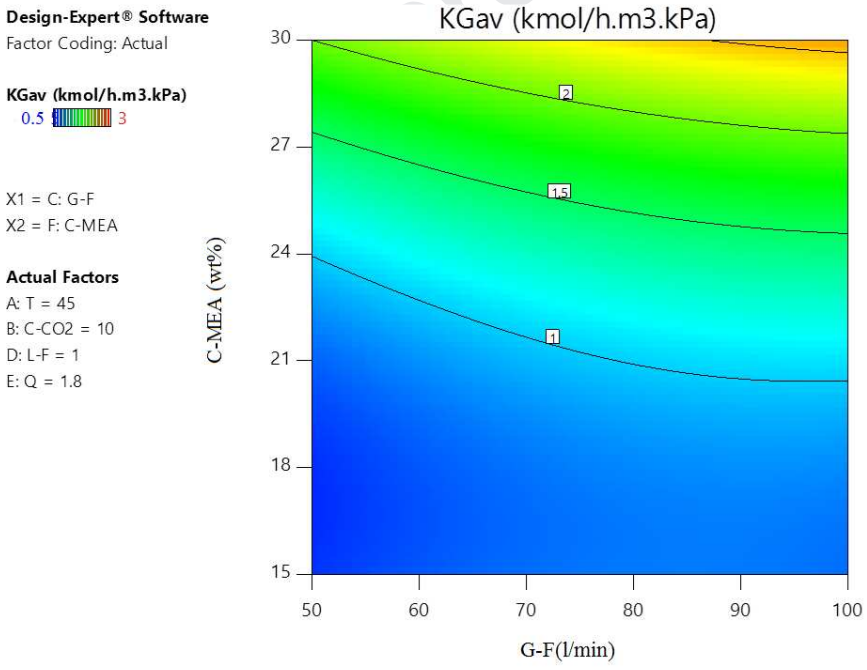

(f)

Fig. 8. The contour plot of the significant interactions for the pair of variables, effect of (a) temperature- amine concentration, (b) temperature-gas flow rate, (c) gas flow rate-reboiler heat duty, (d) inlet CO_2 concentration - amine concentration, (e) reboiler heat duty - amine concentration, (f) gas flow rate - amine concentration on the $K_G a_V$ for MEA-H_2O.

Figs. 9a and c both indicate the enhancement in the $K_G a_V$ value for MEA-MeOH, by increasing in the initial amine concentration to 30 wt%, at low values of temperature and/or CO_2 concentration. The interactions between the inlet gas flow rates and the inlet solvent temperature have been demonstrated in Fig. 9b. According to the figure, the temperature rise at high gas flow rates and/or the temperature decline at low gas flow rates, both significantly provide high values of the $K_G a_V$. While circular plots detect the evidence of negligible interactions, the elliptical contour plots in Fig. 9c and d infer that the interactions between process variables, including the inlet CO_2 concentration/amine concentration, and also the reboiler heat duty/amine concentration are significant [60]. The minimum predicted value for the $K_G a_V$ has been illustrated by the surface confined in the smallest ellipse in the contour diagram.

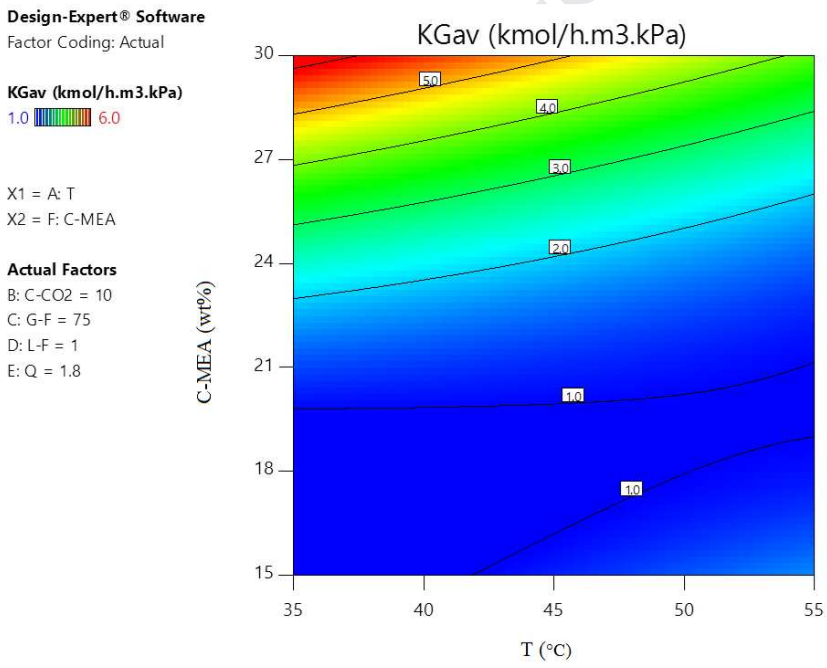

(a)

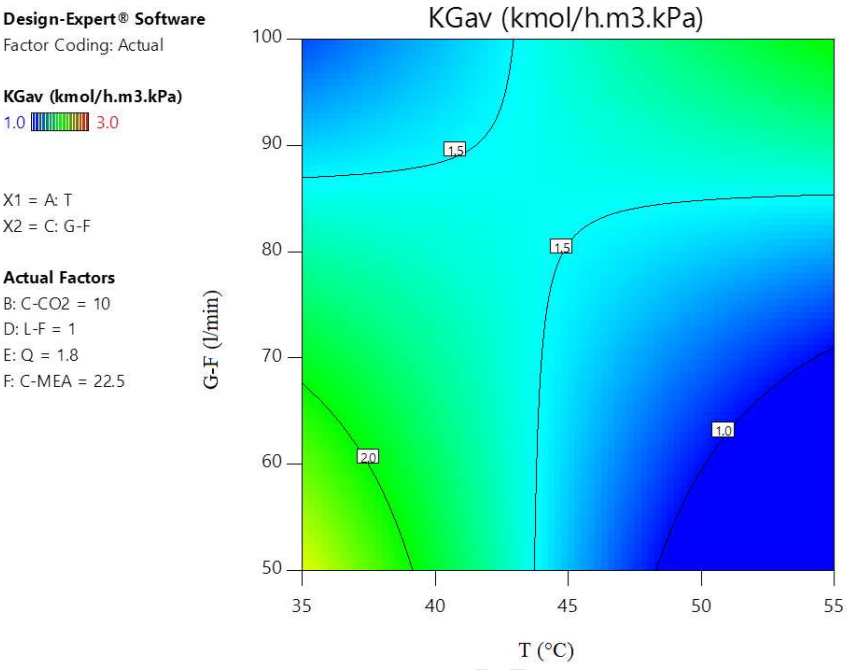
Design-Expert® Software
Factor Coding: Actual
KGav (kmol/h.m3.kPa)
1.0 3.0
X1 = A: T
X2 = C: G-F
Actual Factors
B: C-CO2 = 10
D: L-F = 1
E: Q = 1.8
F: C-MEA = 22.5
KGav (kmol/h.m3.kPa)
G-F (l/min)
T (°C)
100
90
80
70
60
50
35
40
45
50
55
1.5
1.5
2.0
1.0

(b)

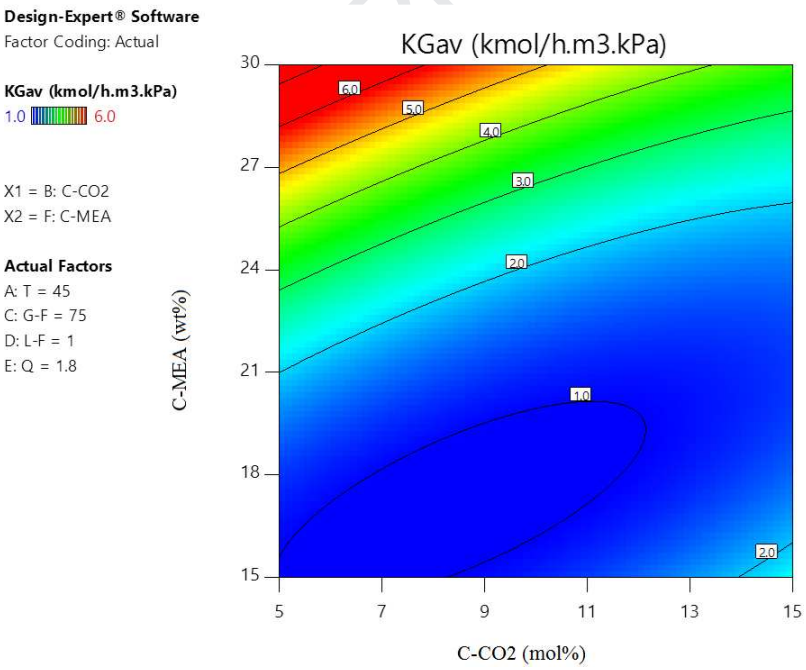
Design-Expert® Software
Factor Coding: Actual
KGav (kmol/h.m3.kPa)
1.0 6.0
X1 = B: C-CO2
X2 = F: C-MEA
Actual Factors
A: T = 45
C: G-F = 75
D: L-F = 1
E: Q = 1.8
KGav (kmol/h.m3.kPa)
C-MEA (wt%)
C-CO2 (mol%)
30
27
24
21
18
15
5
7
9
11
13
15
6.0
5.0
4.0
3.0
2.0
1.0
2.0

(c)

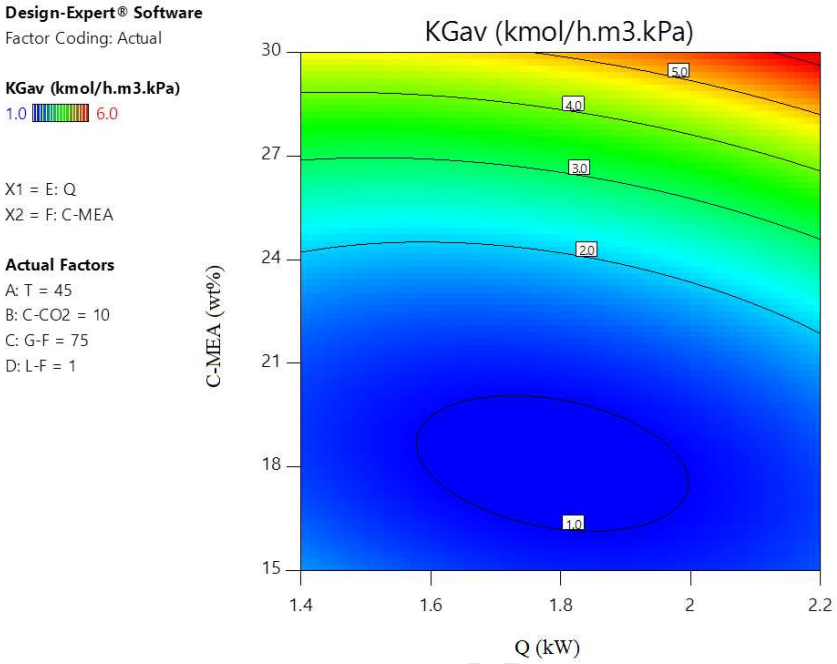

(d)

Fig. 9. The contour plot of the significant interactions for the pair of variables, effects of (a) temperature- amine concentration, (b) temperature-gas flow rate, (c) inlet CO_2 concentration - amine concentration, (d) reboiler heat duty - amine concentration on the $K_G a_V$ for MEA-MeOH.

3.7. Optimization of the process

There are some obvious drawbacks on the above-mentioned analysis, especially in the energy requirement terms. This means that the maximum gas-phase volumetric overall mass transfer coefficient cannot individually justify the proper operating parameters for the absorption and operating cost of an operational amine plant.

The reboiler heat duty (Q_{reg}) for solvent regeneration, which accounts for more than two-thirds of the total operational costs, is an extremely important parameter for evaluating solvent performance [61]. The obtained reboiler heat duty values are high due to the smallscale of laboratory stand. The reason for that is a relatively high percentage of heat loss in overall heat duty [62]. Regarding this, the reboiler heat duty is recognized as the most energy intensive unit. A multiobjective numerical optimization of the process variables was ultimately utilized to

simultaneously maximize the absorption percentage (Φ), and overall gas-phase mass transfer coefficient ($K_G a_V$), along with minimizing the energy consumption (Ω) under the specified optimum condition. The desirability of the optimal solutions is setting as 1.0 to represent the accuracy between the experimental results and suggested model. The optimum condition has been tabulated in Table 5.

Table 5. The predicted optimum condition for MEA-H_2O, and MEA-MeOH.

Factor	Maximum $K_G a_V$		Optimum	
	MEA-H_2O	MEA-MeOH	MEA-H_2O	MEA-MeOH
Temperature (°C)	45	45	45	45
Solvent flow rate (l/min)	1.25	1.25	1.25	1.25
Gas flow rate (l/min)	100	100	100	100
Reboiler heat duty (kW)	2.2	2.2	1.4	1.4
MEA concentration (wt%)	30	30	30	30
Inlet CO_2concentration (mol%)	5	5	15	15

Interestingly, the same operating conditions were obtained for both blended mixtures. Based on the table, the predicted optimum condition to maximize $K_G a_V$ for MEA-H_2O, and MEA-MeOH is the operating temperature of 45 °C, the solvent flow rate of 1.25 l/min, the gas flow rate of 100 l/min, the reboiler heat duty of 2.2 kW, the MEA concentration of is 30 wt%, and the inlet CO_2 concentration of 5 mol%, corresponding to the maximum achieved $K_G a_V$ of 4.30 and 4.98 kmol/h.m^3.kPa. This means that adding methanol solution to the aqueous solution of MEA can enhance the $K_G a_V$ by 15.81 % [40].

The confirmatory experiments showed the values of 4.42 and 5.07 kmol/h.m^3.kPa for MEA-H_2O, and MEA-MeOH under optimal conditions, representing the accuracy of the suggested model. It is worthy to notice that although the process variables of the current study have been defined based on industrial constraints and real requirements, the available optimization covers a narrow range of operating conditions. As such, their extrapolation' will probably lead to very doubtful values.

Finally, the values of the mass transfer coefficient obtained in different experimental works were compared in Table 6. As seen, although the performance of the absorption process in the chemical absorption depends on the defined operating condition, the variation in process parameters cannot alter the order of the obtained values for $K_G a_V$.

Table 6. Comparison of different experimental $K_G a_V$ values, obtained from CO_2 absorption into solution of MEA-MeOH in the packed column.

	Fu et al. [25]	Gao et al. [27]	This work
Temperature (°C)	9.8-12	30-40	35-45
Solvent flow rate (l/h)	1.80-9.90	20-45	45-75
Gas flow rate (m^3/h)	0.34-0.88	2-6	3-6
MEA concentration (wt%)	15-30	30	15-30
Inlet CO_2 concentration (vol%)	6.6-13.8	15	5-15
$K_G a_V$ (kmol/h.m^3.kPa)	0.2-3.3	0.5-3.5	0.95-4.85

Fig. 10 compares the values of the absorption percentage (Φ), the overall gas-phase mass transfer coefficient ($K_G a_V$), and energy consumption (Ω) obtained for MEA-MeOH with that of aqueous MEA solution, which is typically known as a base solvent to capture CO_2. It is found that under the predicted optimum operating conditions, the values of the absorption percentage (Φ) are largely dependent on the type of blended solution, as MEA-MeOH offered the greater absorption percentage of 99.3 %, while that for MEA-H_2O was 91 %. Additionally, for a given CO_2 removal target, the energy consumption using MEA-MeOH would be approximately 3.18 MJ/kg CO_2, while the MEA-H_2O required 3.62 MJ/kg CO_2 energy for removing CO_2, suggesting that methanol based solutions reduce the energy consumption by 12%.

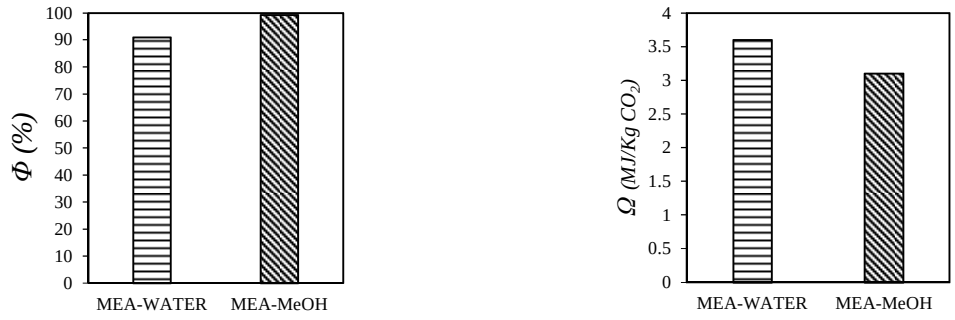

(a) (b)

Fig. 10. Comparision results of (a) the absorption percentage, (b) energy consumption under the optimum condition for MEA-H_2O and MEA-MeOH

4. Conclusion:

Carbon dioxide absorption experiments were conducted by hybrid MEA-H_2O and MEA-MeOH solvents in the absorption/desorption packed column, operating under atmospheric pressure. To assess the MEA-MeOH's potential for CO_2 absorption, the absorption performance were quantified in terms of the gas-phase volumetric overall mass transfer coefficient.

The parametric analysis on the CO_2 absorption efficiency implied that both MEA-H_2O and MEA-MeOH could provide nearly a similar trend for improving the gas-phase volumetric overall mass transfer coefficient with increasing the solvent flow rate, reboiler heat duty, inlet gas flow rate, and MEA concentration. However, increase in the temperature will either have positive or negative effect, depending on the type of blended solution. In addition, the increase in CO_2 concentration in the inlet gas brings adverse consequences on the gas-phase volumetric overall mass transfer coefficient. The details of intensification effects by interactive terms on the process behavior were also discussed in detail.

To provide a comprehensive description on the unit economy, for each amine-blended solution, the values of the gas-phase volumetric overall mass transfer coefficient, the absorption percentage, and energy consumption were simultaneously optimized in terms of the key process variables. Under optimal operating conditions, including temperature of 45 (°C), solvent flow rate of 1.25 (l/min), gas flow rate of 100 (l/min), reboiler heat duty of 1.4 (kW), MEA concentration of 30 (wt%), and inlet CO_2 concentration of 15 (mol%), MEA-MeOH offered a

greater absorption percentage of 99.3 %, while that for MEA-H_2O was 91 %. Additionally, it was recognized that for the given CO_2 removal target, the regeneration energy consumption in the blended solution of MEA-MeOH would be less than the required energy for the MEA-H_2O. It suggests that methanol based solutions play an essential role in controlling the absorption performance and subsequently require low energy for solvent regeneration in cost-effective capture units. Additionally, adding methanol solution to the aqueous solution of MEA could enhance the absorption percentage (Φ) by 9.1, whereas it reduced the energy consumption by 12%.

Acknowledgments

Authors would like to acknowledge the financial support of Kermanshah University of Technology for this research under Grant Number S/P/T/1193.

Nomenclature

a_v	effective interfacial area per unit of packing (m^2/m^3)
C	concentration
F	flow rate (l/min)
G	the inlet gas flow rate (kmol/h.m^2)
$K_G a_V$	the gas-phase volumetric overall mass transfer coefficient (kmol/m^3.h.kPa)
L	inlet liquid flow rate (kmol/h.m^2)
m	the CO_2 captured (kg)
n	the number of independent variables
$\dot{n}$	the molar flow of the gas
P	the system pressure (kPa)
X	independent actual/uncoded variable
y	the mole fraction of CO_2
Y	the mole ratio (mol/mol)
Y	the predicted response
Q	the energy consumed by the reboiler (MJ)
R^2	coefficient of determination
T	temperature (°C)
Z	the height of absorption bed (m)

Greek letters

β	regression coefficients
Φ	the absorption percentage
Ω	the energy consumption of the regenerator

Superscript

0	constant term
i	linear term
ii	quadratic term
ij	interaction term
in	inlet stream
out	outlet stream

Abbreviations and acronyms

ANOVA	Analysis of Variance
BBD	Box-Behnken Design
C-CO_2	inlet CO_2 Concentration (mol%)
C-MEA	amine concentration (wt%)
DF	Degree of Freedom
G-F	Gas Flow rate (l/min)
GHG	Greenhouse Gas
L-F	Liquid Flow rate (l/min)

MEA	Monoethanolamine
MeOH	Methanol
MS	Mean Squares
NOAA	Atmospheric Administration
RSM	Response Surface Methodology
SS	Sum of Squares

References:

[1] Tan L, Shariff A, Lau K, Bustam M. Factors affecting CO_2 absorption efficiency in packed column: a review. Journal of Industrial and Engineering Chemistry. 2012;18(6):1874-83.
[2] Hemmati A, Rashidi H, Behradfar K, Kazemi A. A comparative study of different mass transfer and liquid hold-up correlations in modeling CO2 absorption with MEA. Journal of Natural Gas Science and Engineering. 2019;62:92-100.
[3] Zhang M, Guo Y. Rate based modeling of absorption and regeneration for CO_2 capture by aqueous ammonia solution. Applied energy. 2013;111:142-52.
[4] Chen PC, Luo YX, Cai PW. CO_2 Capture Using Monoethanolamine in a Bubble-Column Scrubber. Chemical Engineering & Technology. 2015;38(2):274-82.
[5] Valeh-e-Sheyda P, Afshari A. A detailed screening on the mass transfer modeling of the CO_2 absorption utilizing silica nanofluid in a wetted wall column. Process Safety and Environmental Protection. 2019;127:125-32.
[6] Tamajón F, Álvarez E, Cerdeira F, Gómez-Díaz D. CO_2 absorption into N-methyldiethanolamine aqueous-organic solvents. Chemical Engineering Journal. 2016;283:1069-80.
[7] Yang H, Xu Z, Fan M, Gupta R, Slimane RB, Bland AE, et al. Progress in carbon dioxide separation and capture: A review. Journal of environmental sciences. 2008;20(1):14-27.
[8] Maqsood K, Mullick A, Ali A, Kargupta K, Ganguly S. Cryogenic carbon dioxide separation from natural gas: a review based on conventional and novel emerging technologies. Reviews in Chemical Engineering. 2014;30(5):453-77.
[9] Kohl AL, Nielsen R. Gas purification: Gulf Professional Publishing, 1997.
[10] Valeh-e-Sheyda P, Rashidi H, Azimi N. Structural improvement of a control valve to prevent corrosion in acid gas treating plant pipeline: An experimental and computational analysis. International Journal of Pressure Vessels and Piping. 2018;165:114-25.
[11] Akbari M, Valeh-e-Sheyda P. CO_2 equilibrium solubility in and physical properties for Monoethanolamine Glycinate at low pressures. Process Safety and Environmental Protection. 2019.
[12] Navaza JM, Gómez-Díaz D, La Rubia MD. Removal process of CO_2 using MDEA aqueous solutions in a bubble column reactor. Chemical Engineering Journal. 2009;146(2):184-8.
[13] Stec M, Tatarczuk A, Więcław-Solny L, Krótki A, Ściążko M, Tokarski S. Pilot plant results for advanced CO2 capture process using amine scrubbing at the Jaworzno II Power Plant in Poland. Fuel. 2015;151:50-6.
[14] Hamborg ES, van Aken C, Versteeg GF. The effect of aqueous organic solvents on the dissociation constants and thermodynamic properties of alkanolamines. Fluid Phase Equilibria. 2010;291(1):32-9.
[15] Hamborg ES, Derks PW, van Elk EP, Versteeg GF. Carbon dioxide removal by alkanolamines in aqueous organic solvents. A method for enhancing the desorption process. Energy Procedia. 2011;4:187-94.
[16] Ramachandran N, Hamborg ES, Versteeg GF. The effect of aqueous alcohols (methanol, t-butanol) and sulfolane on the dissociation constants and thermodynamic properties of alkanolamines. Fluid Phase Equilibria. 2013;360:36-43.
[17] Henni A, Maham Y, Tontiwachwuthikul P, Chakma A, Mather AE. Densities and viscosities for binary mixtures of N-methyldiethanolamine+ triethylene glycol monomethyl ether from 25 C to 70 C and

N-methyldiethanolamine+ ethanol mixtures at 40 C. Journal of Chemical & Engineering Data. 2000;45(2):247-53.
[18] Henni A, Mather AE. Solubility of carbon dioxide in methyldiethanolamine+ methanol+ water. Journal of Chemical and Engineering Data. 1995;40(2):493-5.
[19] Park S-W, Lee J-W, Choi B-S, Lee J-W. Absorption of carbon dioxide into non-aqueous solutions ofN-methyldiethanolamine. Korean Journal of Chemical Engineering. 2006;23(5):806-11.
[20] Álvarez E, Gómez-Díaz D, La Rubia MD, Navaza JM, Pacheco R, Sánchez S. Density and speed of sound of binary mixtures of N-methyldiethanolamine and triethanolamine with ethanol. Journal of Chemical & Engineering Data. 2007;52(5):2059-61.
[21] Idem R, Wilson M, Tontiwachwuthikul P, Chakma A, Veawab A, Aroonwilas A, et al. Pilot plant studies of the CO2 capture performance of aqueous MEA and mixed MEA/MDEA solvents at the University of Regina CO2 capture technology development plant and the boundary dam CO_2 capture demonstration plant. Industrial & engineering chemistry research. 2006;45(8):2414-20.
[22] Naami A, Sema T, Edali M, Liang Z, Idem R, Tontiwachwuthikul P. Analysis and predictive correlation of mass transfer coefficient KGav of blended MDEA-MEA for use in post-combustion CO2 capture. International Journal of Greenhouse Gas Control. 2013;19:3-12.
[23] Versteeg GF, van Swaaij WPM. On the kinetics between CO_2 and alkanolamines both in aqueous and non-aqueous solutions—II. Tertiary amines. Chemical Engineering Science. 1988;43(3):587-91.
[24] Archane A, Gicquel L, Provost E, Fürst W. Effect of methanol addition on water–CO_2–diethanolamine system: Influence on CO_2 solubility and on liquid phase speciation. chemical engineering research and design. 2008;86(6):592-9.
[25] Fu K, Rongwong W, Liang Z, Na Y, Idem R, Tontiwachwuthikul P. Experimental analyses of mass transfer and heat transfer of post-combustion CO_2 absorption using hybrid solvent MEA–MeOH in an absorber. Chemical Engineering Journal. 2015;260:11-9.
[26] Sema T, Naami A, Usubharatana P, Wang X, Gao R, Liang Z, et al. Mass transfer of CO_2 absorption in hybrid MEA-methanol solvents in packed column. Energy Procedia. 2013;37:883-9.
[27] Gao J, Yin J, Zhu F, Chen X, Tong M, Kang W, et al. Integration study of a hybrid solvent MEA-Methanol for post combustion carbon dioxide capture in packed bed absorption and regeneration columns. Separation and Purification Technology. 2016;167:17-23.
[28] Gao J, Yin J, Zhu F, Chen X, Tong M, Kang W, et al. Experimental study of a hybrid solvent MEA-Methanol for post-combustion CO_2 absorption in an absorber packed with three different packing: Sulzer BX500, Mellapale Y500, Pall rings 16× 16. Separation and Purification Technology. 2016;163:23-9.
[29] Gao J, Yin J, Zhu F, Chen X, Tong M, Kang W, et al. Orthogonal test design to optimize the operating parameters of a hybrid solvent MEA–Methanol in an absorber column packed with three different packing: Sulzer BX500, Mellapale Y500 and Pall rings 16×16 for post-combustion CO_2 capture. Journal of the Taiwan Institute of Chemical Engineers. 2016;68:218-23.
[30] Tamajón FJ, Álvarez E, Cerdeira F, Gómez-Díaz D. CO_2 absorption into N-methyldiethanolamine aqueous-organic solvents. Chemical Engineering Journal. 2016;283:1069-80.
[31] Usubharatana P, Tontiwachwuthikul P. Enhancement factor and kinetics of CO2 capture by MEA-methanol hybrid solvents. Energy Procedia. 2009;1(1):95-102.
[32] Usubharatana P. A study of monoethanolamine-methanol hybrid solvents for carbon dioxide capture by absorption: University of Regina (Canada), 2009.
[33] Sema T, Naami A, Usubharatana P, Wang X, Gao R, Liang Z, et al. Mass transfer of CO_2 absorption in hybrid MEA-methanol solvents in packed column. Energy Procedia. 2013;37(0):883-9.
[34] Abu-Zahra MR, Schneiders LH, Niederer JP, Feron PH, Versteeg GF. CO_2 capture from power plants: Part I. A parametric study of the technical performance based on monoethanolamine. International Journal of Greenhouse gas control. 2007;1(1):37-46.
[35] Mahajani V, Joshi J. Kinetics of reactions between carbon dioxide and alkanolamines. Gas Separation & Purification. 1988;2(2):50-64.

[36] Versteeg G, Van Dijck L, van Swaaij WPM. On the kinetics between CO_2 and alkanolamines both in aqueous and non-aqueous solutions. An overview. Chemical Engineering Communications. 1996;144(1):113-58.
[37] Sema T, Naami A, Fu K, Edali M, Liu H, Shi H, et al. Comprehensive mass transfer and reaction kinetics studies of CO_2 absorption into aqueous solutions of blended MDEA–MEA. Chemical engineering journal. 2012;209:501-12.
[38] Vaidya PD, Kenig EY. CO2-Alkanolamine reaction kinetics: A review of recent studies. Chemical Engineering & Technology. 2007;30(11):1467-74.
[39] Rayer AV, Henni A, Li J. Reaction kinetics of 2-((2-aminoethyl) amino) ethanol in aqueous and non-aqueous solutions using the stopped-flow technique. The Canadian Journal of Chemical Engineering. 2013;91(3):490-8.
[40] Sahraie S, Rashidi H, Valeh-e-Sheyda P. An optimization framework to investigate the CO_2 capture performance by MEA: Experimental and statistical studies using Box-Behnken design. Process Safety and Environmental Protection. 2019;122:161-8.
[41] Zeng Q, Guo Y, Niu Z, Lin W. Mass transfer coefficients for CO_2 absorption into aqueous ammonia solution using a packed column. Industrial & Engineering Chemistry Research. 2011;50(17):10168-75.
[42] Körbahti BK, Tanyolaç A. Continuous electrochemical treatment of simulated industrial textile wastewater from industrial components in a tubular reactor. Journal of Hazardous Materials. 2009;170(2):771-8.
[43] Sadri Moghaddam S, Alavi Moghaddam MR, Arami M. Coagulation/flocculation process for dye removal using sludge from water treatment plant: Optimization through response surface methodology. Journal of Hazardous Materials. 2010;175(1):651-7.
[44] Rezazadeh F. Optimal Integration of Post-Combustion CO_2 Capture Process with Natural Gas Fired Combined Cycle Power Plants: University of Leeds, 2016.
[45] Nittaya T, Douglas PL, Croiset E, Ricardez-Sandoval LA. Dynamic modelling and control of MEA absorption processes for CO2 capture from power plants. Fuel. 2014;116:672-91.
[46] Bui M, Gunawan I, Verheyen TV, Meuleman E, Feron P. Dynamic operation of post-combustion CO2 capture in Australian coal-fired power plants. Energy Procedia. 2014;63:1368-75.
[47] Xue B, Yu Y, Chen J, Luo X, Wang M. A comparative study of MEA and DEA for post-combustion CO2 capture with different process configurations. International Journal of Coal Science & Technology. 2017;4(1):15-24.
[48] Versteeg GF, Van Dijck LAJ, Van Swaaij WPM. On The Kinetics Between CO_2 And Alkanolamines Both In Aqueous And Non-Aqueous Solutions. An Overview. Chemical Engineering Communications. 1996;144(1):113-58.
[49] Koneripalli N, Tekie Z, Morsi BI, Chang M-Y. Mass transfer characteristics of gases in methanol and ethanol under elevated pressures and temperatures. The Chemical Engineering Journal and the Biochemical Engineering Journal. 1994;54(2):63-77.
[50] Ahmadi H. Measurement and Modeling of Carbon Dioxide Solubility in Polar and Nonpolar Solvent. Research Journal of Applied Sciences, Engineering and Technology. 2012;4(15):2357-60.
[51] Ermatchkov V, Pérez-Salado Kamps Á, Maurer G. Solubility of carbon dioxide in aqueous solutions of N-methyldiethanolamine in the low gas loading region. Industrial & engineering chemistry research. 2006;45(17):6081-91.
[52] Aroonwilas A, Tontiwachwuthikul P, Chakma A. Effects of operating and design parameters on CO_2 absorption in columns with structured packings. Separation and Purification Technology. 2001;24(3):403-11.
[53] Zeng Q, Guo Y, Niu Z, Lin W. The absorption rate of CO_2 by aqueous ammonia in a packed column. Fuel processing technology. 2013;108:76-81.
[54] Rahmandoost E, Roozbehani B, Maddahi MH. Experimental studies of CO_2 capturing from the flue gases. Iranian Journal of Oil & Gas Science and Technology. 2014;3(4):1-15.
[55] Hemmati A, Rashidi H. Mass transfer investigation and operational sensitivity analysis of amine-based industrial CO_2 capture plant. Chinese Journal of Chemical Engineering. 2018.

[56] Hemmati A, Rashidi H. Optimization of industrial intercooled post-combustion CO_2 absorber by applying rate-base model and response surface methodology (RSM). Process Safety and Environmental Protection. 2019;121:77-86.
[57] Valeh-e-Sheyda P, Rashidi H. Inhibition of corrosion in amine air cooled heat exchanger: Experimental and numerical study. Applied Thermal Engineering. 2016;98:1241-50.
[58] Rashidi H, Valeh-e-Sheyda P. An insight on amine air-cooled heat exchanger tubes' corrosion in the bulk CO2 removal plant. International Journal of Greenhouse Gas Control. 2016;47:101-9.
[59] White L, Street D. Corrosion control in amine treating units. Conference Corrosion control in amine treating units. p. 17-8.
[60] Muralidhar R, Gummadi SN, Dasu VV, Panda T. Statistical analysis on some critical parameters affecting the formation of protoplasts from the mycelium of Penicillium griseofulvum. Biochemical Engineering Journal. 2003;16(3):229-35.
[61] Liang Z, Fu K, Idem R, Tontiwachwuthikul P. Review on current advances, future challenges and consideration issues for post-combustion CO2 capture using amine-based absorbents. Chinese Journal of Chemical Engineering. 2016;24(2):278-88.
[62] Wilk A, Więcław-Solny L, Tatarczuk A, Krótki A, Spietz T, Chwoła T. Solvent selection for CO_2 capture from gases with high carbon dioxide concentration. Korean Journal of Chemical Engineering. 2017;34(8):2275-83.

Highlights:

- A rigorous process model was developed for a hybrid physical-chemical solvent for CO_2 absorption process.
- Adding methanol to an aqueous MEA markedly lowers the regeneration energy consumption by 12%.
- Adding methanol to an aqueous MEA augments the CO_2 absorption percentage (Φ) by 9.1 %.
- Under optimal operating conditions, MEA-H_2O offered an absorption percentage of 91 %.
- Under optimal operating conditions, MEA-MeOH offered an absorption percentage of 99.3 %.

Declaration of interests

☐ The authors declare that they have no known competing financial interests or personal relationships that could have appeared to influence the work reported in this paper.

☒The authors declare the following financial interests/personal relationships which may be considered as potential competing interests:

Acknowledgments
Authors would like to acknowledge the financial support of Kermanshah University of Technology for this research under Grant Number S/P/T/1193.